



Calhoun: The NPS Institutional Archive
DSpace Repository

Theses and Dissertations

1. Thesis and Dissertation Collection, all items

1974-03

Iterative retrieval and statistical specification
of atmospheric thicknesses from VTPR
clear-column radiance data

Moran, Douglas Ray

Monterey, California. Naval Postgraduate School

<http://hdl.handle.net/10945/40308>

This publication is a work of the U.S. Government as defined in Title 17, United States Code, Section 101. Copyright protection is not available for this work in the United States.

Downloaded from NPS Archive: Calhoun



Calhoun is the Naval Postgraduate School's public access digital repository for research materials and institutional publications created by the NPS community. Calhoun is named for Professor of Mathematics Guy K. Calhoun, NPS's first appointed -- and published -- scholarly author.

Dudley Knox Library / Naval Postgraduate School
411 Dyer Road / 1 University Circle
Monterey, California USA 93943

<http://www.nps.edu/library>

NAVAL POSTGRADUATE SCHOOL

Monterey, California



THESIS

ITERATIVE RETRIEVAL AND STATISTICAL
SPECIFICATION OF ATMOSPHERIC THICKNESSES
FROM VTPR CLEAR-COLUMN RADIANCE DATA

by

Douglas Ray Moran

Thesis Advisor:

F.L. Martin

March 1974

Thesis
M8185

Approved for public release; distribution unlimited.

NAVAL POSTGRADUATE SCHOOL

Monterey, California



THESIS

ITERATIVE RETRIEVAL AND STATISTICAL
SPECIFICATION OF ATMOSPHERIC THICKNESSES
FROM VTPR CLEAR-COLUMN RADIANCE DATA

by

Douglas Ray Moran

Thesis Advisor:

F.L. Martin

March 1974

Approved for public release; distribution unlimited.

Iterative Retrieval and Statistical
Specification of Atmospheric Thicknesses
from VTPR Clear-Column Radiance Data

by

Douglas Ray Moran
Lieutenant, United States Navy
B.S., Michigan State University, 1967

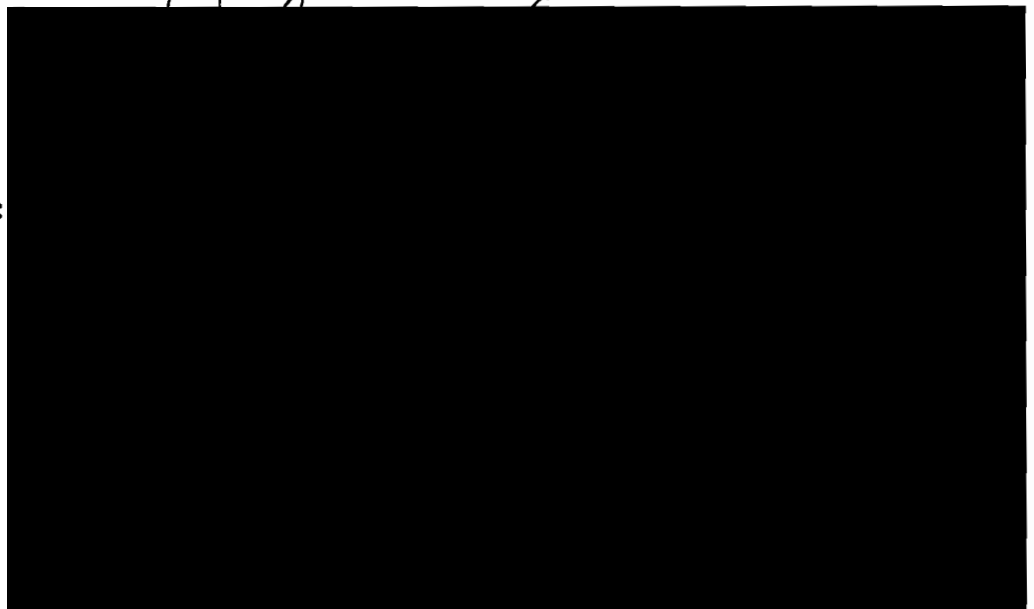
Submitted in partial fulfillment of the
requirements for the degree of

MASTER OF SCIENCE IN METEOROLOGY

from the
NAVAL POSTGRADUATE SCHOOL
March 1974

Author

Approved by:



ABSTRACT

An iterative technique is developed for retrieval of thicknesses of selected atmospheric layers from VTPR "clear-column" radiance measurements. Layer mean temperatures for a simplified atmospheric model are retrieved by direct solution of the radiative transfer equation, and are then used to compute thicknesses of key atmospheric layers bounded by commonly used pressure levels. The retrieval technique illustrates the use of reference wave numbers that vary from layer to layer. Transmittance tuning is employed to correct systematic errors in the retrieved mean temperatures. Thicknesses of key layers retrieved by the technique from "clear-column" radiances observed during a 24 hour period at scan spots between 15 N and 45 N are separated into three latitude-band samples. Each sample is subjected to stepwise multiple regression analysis to determine the thickness-specification of various standard layers in terms of the clear column radiances. RMS error-analyses resulting from the regression are then used to determine the quality of thickness-specifications of simulated tropospheres and stratospheres.

TABLE OF CONTENTS

I.	INTRODUCTION -----	10
II.	SATELLITE DATA -----	15
III.	RETRIEVAL TECHNIQUE -----	23
	A. MATHEMATICAL DEVELOPMENT -----	23
	B. APPLICATION -----	30
	1. Program Input Parameters -----	30
	a. First Guess Temperature Profiles -	30
	b. Atmospheric Transmittance Values -	31
	2. Computational Procedure -----	32
	a. Mean Temperature Retrieval -----	32
	b. Standard-Layer Thickness Calculation -----	33
IV.	EVALUATION OF RETRIEVAL ACCURACY -----	35
V.	TRANSMITTANCE TUNING -----	40
VI.	RETRIEVED THICKNESS ANALYSIS -----	44
	A. INDIVIDUAL LAYER SPECIFICATION -----	44
	1. Stepwise Regression Analysis -----	44
	2. Individual Layer Results -----	47
	B. TROPOSPHERIC SPECIFICATION BY SUB-LAYERS -	51
	1. Method of Analysis -----	52
	2. Troposphere Results -----	55
	C. STRATOSPHERIC SPECIFICATION BY SUB-LAYERS	62
	1. Method of Analysis -----	62
	2. Stratosphere Results -----	62
VII.	CONCLUSIONS -----	71

APPENDIX A Climatological Temperature Profiles -----	72
APPENDIX B Carbon Dioxide Transmittances -----	74
COMPUTER PROGRAM and SAMPLE OUTPUT	
Mean Temperature Retrieval -----	77
COMPUTER PROGRAM and SAMPLE OUTPUT	
Thickness Calculation -----	84
LIST OF REFERENCES -----	87
INITIAL DISTRIBUTION LIST -----	89
FORM DD 1473 -----	90

LIST OF TABLES

1.	VTPR channels, half-widths, and central wave numbers -----	17
2.	Scan spot samples for analysis of retrieved thickness data -----	44
3.	Statistical parameters of representative sequential layers -----	49
4.	Statistical parameters of layers of special interest -----	50
5.	Tropospheric sub-layer combinations having the smallest error index values -----	57
6.	Error index values for defined "tropospheres" --	58
7.	Stratospheric sub-combinations having the smallest error index values -----	65
8.	Error index values for defined "stratospheres" --	66

LIST OF FIGURES

1.	Exact vs. calculated rectangular function -----	12
2.	Satellite tracks for NOAA-II VTPR coverage -----	16
3.	VTPR scan pattern and data analysis array -----	19
4.	Procedure for determining "clear-column" radiances -----	21
5.	Seventeen layer atmosphere model -----	26
6.	Tuned and untuned temperature retrievals, 17.5 N	38
7.	Tuned and untuned temperature retrievals, 43.1 N	39
8.	Weighting functions for VTPR carbon dioxide channels -----	42
9.	Combinations of tropospheric sub-layers formed by 400 mb sliding layer -----	54
10.	Tropospheric sub-layer combinations and E.I. values, 15 N to 25 N -----	59
11.	Tropospheric sub-layer combinations and E.I. values, 25 N to 35 N -----	60
12.	Tropospheric sub-layer combinations and E.I. values, 35 N to 45 N -----	61
13.	Combinations of stratospheric sub-layers formed by 30 mb sliding layer -----	63
14.	Stratospheric sub-layer combinations and E.I. values, 15 N to 25 N -----	68
15.	Stratospheric sub-layer combinations and E.I. values, 25 N to 35 N -----	69
16.	Stratospheric sub-layer combinations and E.I. values, 35 N to 45 N -----	70

TABLE OF SYMBOLS AND ABBREVIATIONS

$B_i[T(p)]$	Planck radiance function for temperature T at pressure level p
$B_i(K)$	Layer mean Planck function for layer K and reference wave number ν_i .
$B_{wtd}(K)$	Weighted layer mean Planck value corresponding to layer reference number $\tilde{\nu}_K$.
E.I.	Error index
F_k	F-ratio upon entry at step k
FNWC	Fleet Numerical Weather Central
gpm	Geopotential meter
I_i	Spectral radiance in channel i
mb	millibar
NESS	National Environmental Satellite Service
NMC	National Meteorological Center
NOAA	National Oceanic and Atmospheric Administration
ν_i	Wave number at center of channel i
$\tilde{\nu}_K$	Reference wave number for layer K
p_o	Pressure at top of the atmosphere (.01 mb)
p_s	Pressure at surface of the earth (1000 mb)
RTE	Radiative transfer equation
S.E.	Standard error of estimate
SIRS	Satellite Infra-Red Spectrometer
SR	Scanning Radiometer
SST	Sea surface temperature
σ	Standard deviation
$\bar{T}(K)$	Mean temperature of layer K

$\tau_1(p)$	Fractional transmittance of atmosphere in channel 1 from level p to p_0
VTPR	Vertical Temperature Profile Radiometer
R	Multiple correlation coefficient

ACKNOWLEDGEMENTS

The author wishes to express his appreciation to Professor Frank L. Martin for his generous assistance and guidance in the research and preparation of this paper.

Appreciation is also expressed to the author's family for patience and understanding during the period of thesis work, and to the staff of the W. R. Church Computer Facility for assistance in computer phases of the research.

I. INTRODUCTION

Retrieval of meteorological parameters from satellite radiance measurements has been the object of numerous research studies since Kaplan [1959] demonstrated that vertical temperature profiles of the atmosphere could be inferred from satellite spectral radiance observations in the 15 μm band of carbon dioxide emission. Application of retrieval techniques to satellite measurements has been possible since the launch of NIMBUS III in 1969 and to date emphasis has been on retrieval of temperature profiles.

However, for purposes of numerical weather prediction, the atmospheric thickness of a specified pressure interval is normally a more basic parameter than temperature [Fleming, 1972]. Furthermore, thicknesses of specific atmospheric pressure intervals, or layers, may be retrieved by direct solution of the radiative transfer equation, thereby eliminating the need for "a priori" statistical information necessary for retrieval by regression or inverse matrix methods [Fritz, Wark, et al., 1972].

A direct retrieval method for obtaining specific layer mean temperatures, and hence thicknesses, from satellite radiance measurements was presented by Fleming [1972]. The method proved to be too time-consuming to be operationally adaptable by the National Environmental Satellite Service (NESS) to the National Meteorological Center (NMC) analysis

scheme as described by McMillin, Wark, et al. [1973], and the retrieved thickness values showed little improvement in accuracy when compared to results obtained by a statistical regression technique which gave a $T(p)$ profile at mandatory levels from which thicknesses were computed [Smith and Fleming, 1972]. However, the concept proposed by Fleming [1972] appeared to have at least diagnostic merit for application to vertical analysis schemes such as that of Fleet Numerical Weather Central (FNWC), which employs a layer thickness as an input parameter [Holl, et al., 1964].

Fleming proposed a method whereby the unit square wave function denoted by $R(\ln p/p_s)$ could be determined as a linear combination of spectral radiances, I_i , with coefficients, c_i , chosen to minimize the right side of

$$\sum_{i=1}^N c_i I_i = \Delta \bar{T} \int_{p_0}^{p_s} R[\ln p/p_s; p_1, p_2] d(\ln p) \quad (1)$$

Here

$\Delta \bar{T}$ = mean temperature for pressure interval (p_1, p_2) .

p_0, p_s = pressures at top of atmosphere and surface of earth.

$i = 1, 2, \dots, N$ are the spectral intervals or channels.

The R -functions were sought to provide, in sequence, exact fits to the square wave in the significant layers of the atmosphere. By Fleming's theory they should ideally fit the square wave of Fig. 1 between p_1 and p_2 and be zero elsewhere along the p -axis.

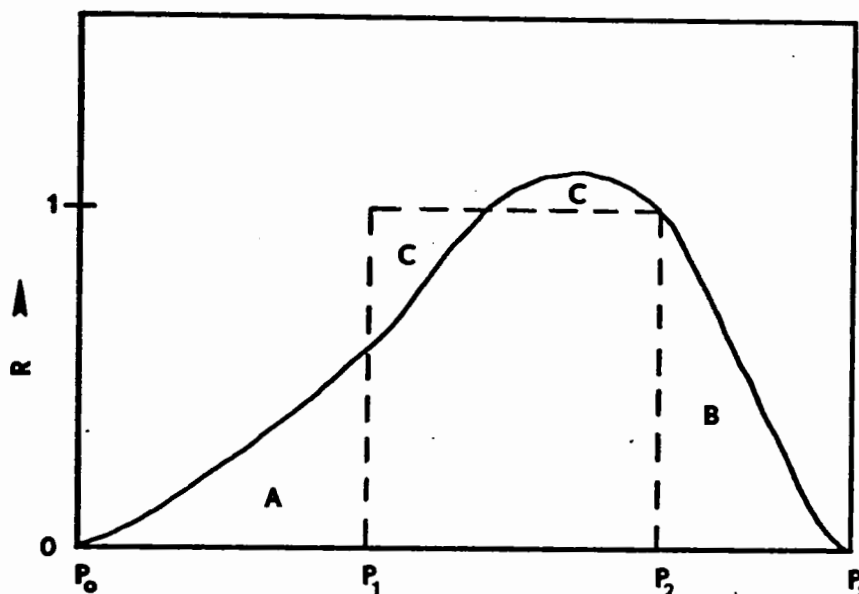


FIG. 1. Exact vs. calculated rectangular function R . Desired solution indicated by dashed line, calculated solution indicated by solid line.

In practice, the calculated R functions did not fit the square wave exactly and left errors in adjacent pressure regions as depicted by areas A and B of Fig. 1. Inexactness of fit at the top of the square wave resulting in area C was considered unimportant because it tended to average out to the required thickness constraint over (p_1, p_2) .

The implication was that the better the R function fits the square wave for a given layer (p_1, p_2) , the better the mean temperature of the layer was specified by the radiance measurements.

The object of this thesis was first to develop a direct retrieval technique for layer-mean temperatures (and therefore thicknesses) which required a minimum of computer time, and could conceivably be less sensitive to channel noise than Fleming's method. A second objective was designed to test retrieved thicknesses for optimum layer specification by statistical methods, as implied by Fleming's square wave concept.

In this thesis a new simplified iterative retrieval technique was developed for use with VTPR "clear-column" radiances to obtain mean temperatures over greater pressure intervals than the mandatory pressure increments used by Fleming. An iterative retrieval technique was used because of the minimum computer time and space required. The use of larger pressure intervals was employed to reduce the effect of channel noise and to improve accuracy, since the accuracy of mean temperatures derived from radiance measurements usually improves with increasing pressure interval [Hayden, 1971].

Key-layer thicknesses derived hypsometrically from the mean $T(p)$ profile were then subjected to stepwise multiple regression analysis to determine which key layer was best specified by the "clear-column" radiances. The troposphere and lower stratosphere were considered separately, that is layers crossing the tropopause level such as 500 to 50 mb were not considered.

Results of the regression analysis were examined first to determine which particular layer in the troposphere (and also which layer in the lower stratosphere) could be used as the most effective thickness from VTPR retrieval for use in the FNWC vertical-structure analysis scheme, which currently makes use of the 1000 to 300 mb thickness in processing of conventional sounding data.

Next, combinations of sub-layers which span the troposphere were examined to determine if a better statistical fit for the retrieved tropospheric thickness could be obtained from the combinations of sub-layers, and if so, then which combination was best. A similar study was made for the lower stratosphere.

II. SATELLITE DATA

The launch of NOAA-II with its Vertical Temperature Profile Radiometer (VTPR) instrument in October, 1972 marked a major improvement in radiance measurement capability. The VTPR instrument is superior to its earlier counterparts, the SIRS-A of NIMBUS III and the SIRS-B of NIMBUS IV, in that it has much better spatial resolution. Sub-satellite dimensions for scans spots are approximately 69 by 67 km for VTPR compared to 225 by 225 km for SIRS-A and SIRS-B. The improved resolution permits more accurate computation of "clear-column" radiances, which are equivalent to radiances that would be observed in completely clear skies. Use of "clear-column" radiances for retrieval eliminates the necessity to correct for cloud cover which was a significant problem in retrieval techniques developed for use with SIRS-A and SIRS-B data.

NOAA-II orbits the earth every 115 minutes at an altitude of 1464 km. Figure 2 illustrates the earth projection of seven orbits. North to south portions of the orbit are indicated by solid lines; south to north portions are indicated by dashed lines. Shaded areas depict areal coverage during two orbits. North to south equator crossings occur at 0900 and south to north crossings occur at 2100 local solar time.

The VTPR instrument scans perpendicular to the satellite path in 23 discrete steps from left to right, representing

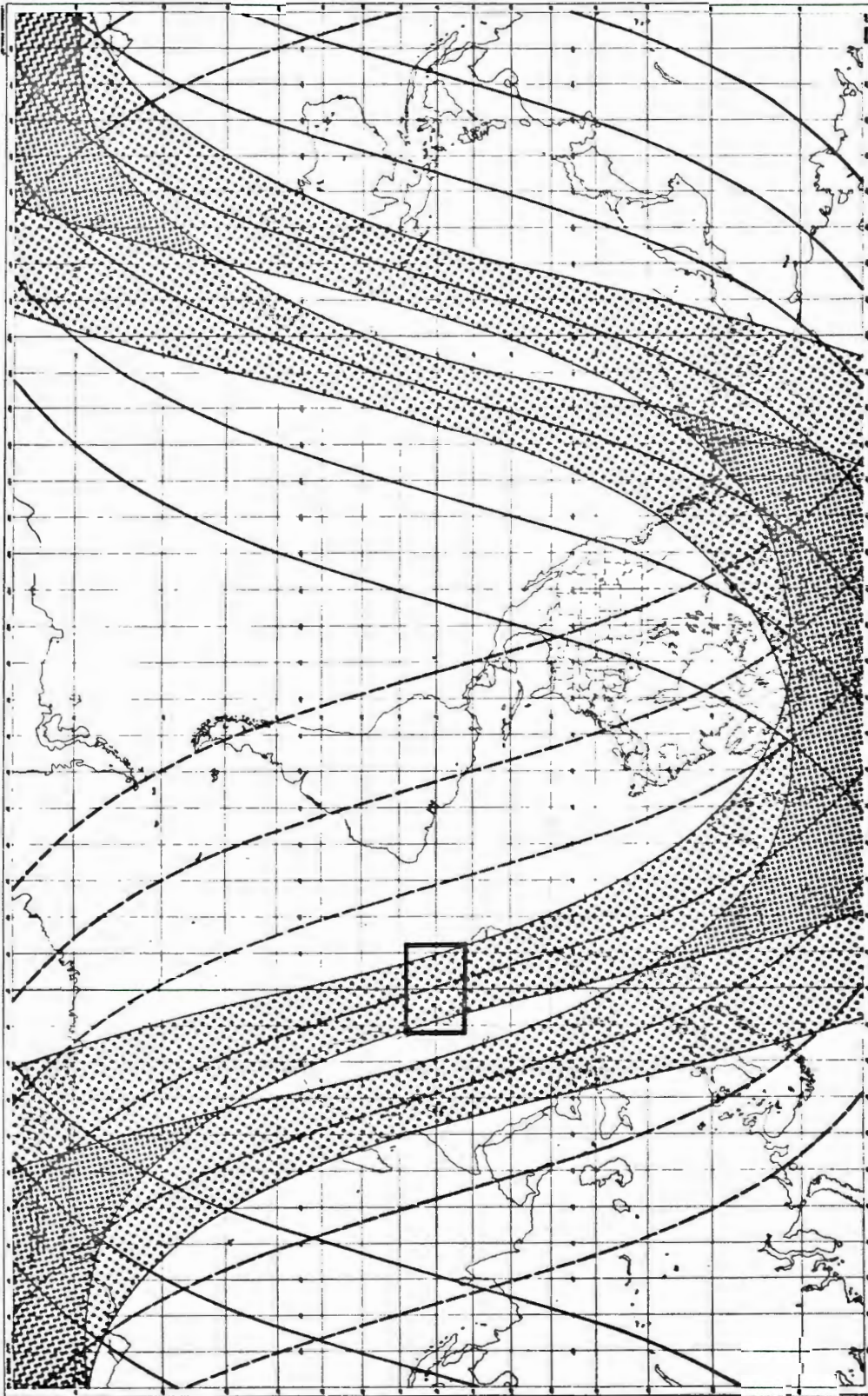


FIG. 2. Satellite tracks for NOAA II VTPR coverage

a scan path of 30.3 degrees both sides of the local nadir. Each step provides a "scan spot" which is observed by the VTPR instrument in six spectral intervals of the 15 μm band of carbon dioxide, in one interval of the 12 μm atmospheric window, and in one interval of the 19 μm water vapor band. The eight spectral intervals, or channels, along with their respective half-widths and central wave numbers are listed in Table 1.

TABLE 1. VTPR channel designators corresponding half-widths, and central wave numbers.

Channel	1	2	3	4	5	6	7	8
Wave No. (ν_1) (cm^{-1})	668.5	677.5	695.0	708.0	725.0	747.0	535.0	835.0
Half-width (cm^{-1})	3.5	10.0	10.0	10.0	10.0	10.0	18.0	10.0

Channels one through six are carbon dioxide channels, channel seven is the water vapor channel, and channel eight is the window channel. Maximum relative measurement error between any two channels except the 668.5 cm^{-1} channel is 0.25 $\text{mW}/(\text{m}^2 \text{ ster } \text{cm}^{-1})$; maximum relative error between the 668.5 cm^{-1} channel and any other channel is 0.75 $\text{mW}/(\text{m}^2 \text{ ster } \text{cm}^{-1})$.

Other instruments aboard NOAA-II include a two-channel Scanning Radiometer (SR) which measures radiances in the 10.4-12.5 and 0.5-0.7 μm intervals. Resolution is more

refined in the SR scan spots than that of the VTPR, with sub-satellite dimensions at the nadir being approximately 7.5 by 7.5 km. Statistical techniques are used to identify scanning radiometer measurements which signify cloud-free areas, and these "clear-column" SR window channel radiances are then used to determine sea surface temperatures for the VTPR scan spots.

Conversion of the VTPR raw radiance measurements to "clear-column" radiances is accomplished by first dividing scan spots into analysis arrays. Scan spots from eight successive scan lines are divided into three boxes, or sub-arrays, of 8 by 8, 8 by 7, and 8 by 8 spots as illustrated in Fig. 3, which is an enlargement of the boxed area outlined in Fig. 2. From the VTPR raw radiance measurements and the SR derived sea surface temperatures of scan spots within each sub-array, a single set of "clear-column" radiances is computed by statistical methods [McMillin, Wark, et al, 1973], and assigned to central scan spot locations indicated by X's in Fig. 3.

The procedure is essentially to compute an 835.0 cm^{-1} window channel radiance by the Planck formula using the sea surface temperature, and to compare the computed value against the measured 835.0 cm^{-1} window channel radiance. If the measured 835.0 cm^{-1} radiance value equals or exceeds the computed value (from the known sea-surface temperature field, denoted by SST), the radiances are considered to be in agreement and the scan spot is assumed to be cloud-free.

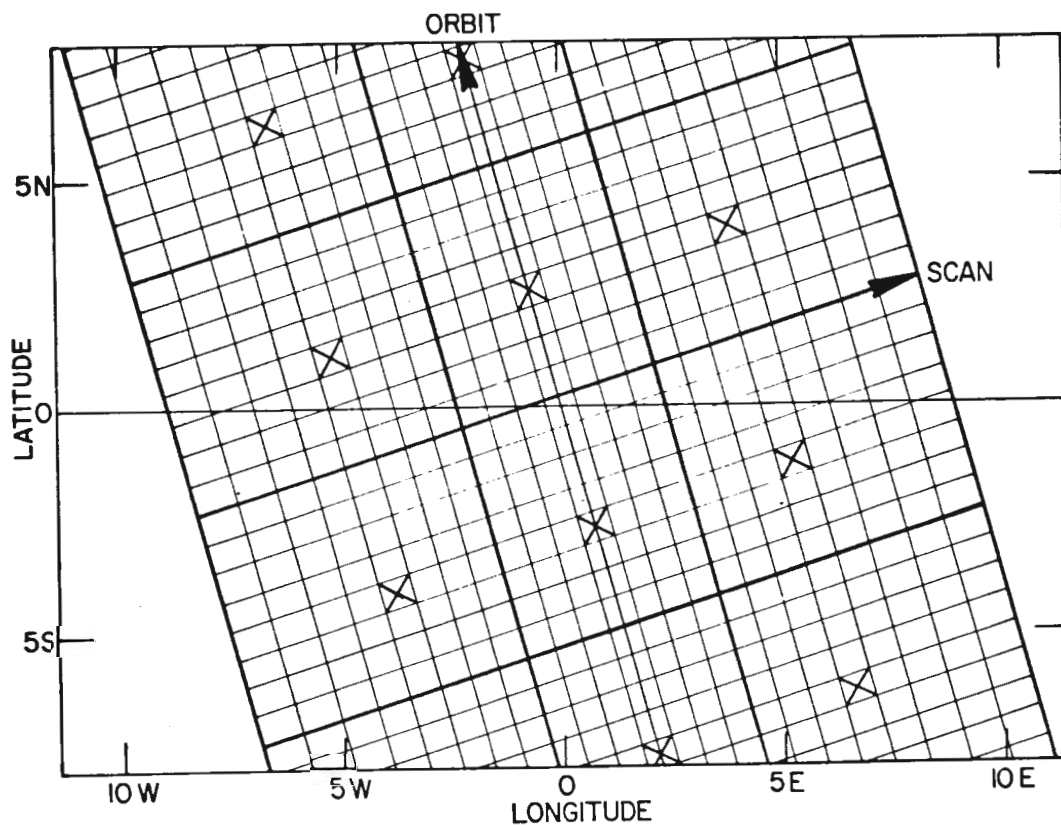


FIG. 3. VTPR scan pattern and data analysis array for the outlined box in Fig. 2.

If the computed value (from the SST) exceeds the measured value, the scan spot is assumed to contain significant cloud cover and equivalent "clear-column" radiance values are calculated by noting that for a given wave number, ν_1 ,

$$\frac{I_{\text{clr}}(\nu_1) - I_2(\nu_1)}{I_{\text{clr}}(\nu_8) - I_2(\nu_8)} = \frac{I_{\text{clr}}(\nu_1) - I_1(\nu_1)}{I_{\text{clr}}(\nu_8) - I_1(\nu_8)} . \quad (2)$$

Here

$I_{\text{clr}}(\nu_8)$ = window radiance computed from the SR derived sea surface temperature.

$I_1(\nu_1), I_2(\nu_1)$ = raw radiances in channel 1 measured at scan spots 1 and 2 having the same sea surface temperature.

$I_{\text{clr}}(\nu_1)$ = desired "clear-column" radiance value for wave number 1.

$I_1(\nu_8), I_2(\nu_8)$ = radiance measured for the 835.0 cm^{-1} window channel at scan spots 1 and 2.

As shown in Fig. 4, the three points $[I_{\text{clr}}(\nu_1), I_{\text{clr}}(\nu_8)]$, $[I_1(\nu_1), I_1(\nu_8)]$, and $[I_2(\nu_1), I_2(\nu_8)]$ lie on the straight line determined from the measured values of $I_1(\nu_1)$, $I_1(\nu_8)$, $I_2(\nu_1)$, and $I_2(\nu_8)$. The slope of this line is expressed by the right side of eq. (2).

The value of $I_{\text{clr}}(\nu_1)$ can then be determined from the known value of $I_{\text{clr}}(\nu_8)$. When computing $I_{\text{clr}}(\nu_1)$ values, radiances from adjacent scan spots with different nadir angles are adjusted to a common zenith angle.

After clear radiance values are obtained for all channels at each scan spot within a sub-array, all values from adjacent scan spots are examined. The sub-array maximum radiance set yields a single set of eight "clear-column" radiances, and a sea surface temperature positioned at the center of the sub-array. This results in reduction of raw radiances for the 184 scan spots of the 8 by 23 analysis array, to "clear-column" radiances at only the centers of the three sub-arrays.

The resulting VTPR "clear-column" radiance values and associated data are recorded on archival tapes. An archival tape for April 12, 1973, was provided for this study through

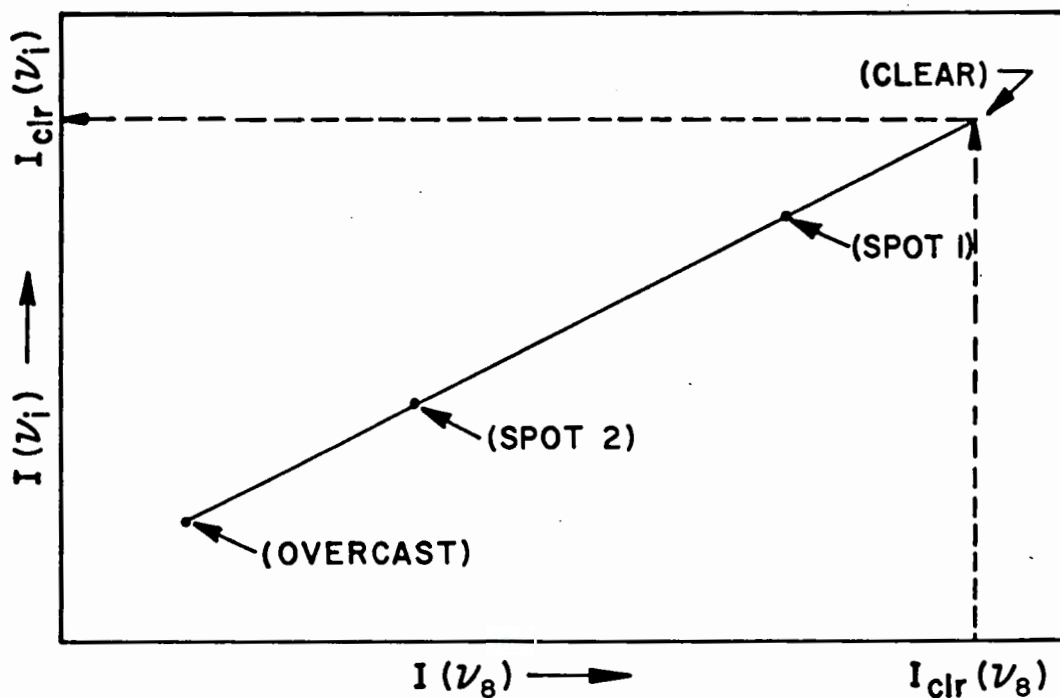


FIG. 4. Procedure for determining "clear-column" radiances.

the kind auspices of Dr. D. Q. Wark of NESS. From a printout of archival file II (the "clear column" file), radiances for the six carbon dioxide channels and the sea surface temperature, as well as the geographic coordinates, were extracted for clear column scan spots between 15 and 45 degrees north latitude.

Data from the tape printout were then transformed to correct dimensions as follows:

N. Latitude in degrees	= (tape value) x .10 - 90
W. Longitude in degrees	= (tape value) x .10
Radiances in $\text{mW}/(\text{m}^2 \text{ ster cm}^{-1})$	= (tape value) x .05
Sea surface temperature in $^{\circ}\text{K}$	= (tape value) x .20 + 269.9

Additional information on characteristics of the NOAA-II satellite and its VTPR and SR radiance data may be found in NOAA technical reports [Fritz, Wark, et al., 1972] and [McMillin, Wark, et al., 1973] from which most of the details of this section were taken.

III. RETRIEVAL TECHNIQUE

Given VTPR "clear-column" radiance values for channels one through six and the sea surface temperature computed essentially from SR measurements, corresponding layer mean temperature profiles were obtained using an iterative technique derived from that initially presented by Smith [1970] and modified by Martin [1973] for the purposes of this study. Mean temperatures are then converted to layer thicknesses by use of the hypsometric equation, as if the mean temperatures of the iterative procedure applied to their central pressure levels.

A. MATHEMATICAL DEVELOPMENT

For a cloudless, non-scattering atmosphere in thermodynamic equilibrium, the spectral radiance observed at the top of the atmosphere for each channel is related to the vertical temperature profile and absorbing gas structure by the radiative transfer equation (RTE) [Fritz, Wark, et al., 1972]:

$$I_1 = B_1[T(p_s)]\tau_1(p_s) + \int_{x(p_s)}^{x(p_o)} B_1[T(p)] \frac{d\tau_1(p)}{dx(p)} dx(p) \quad (3)$$

(A)

(B)

where

I_1 = spectral radiance in channel 1, ($i=1,2,\dots,6$),

$B_1[T(p)]$ = Planck radiance function for channel 1 and temperature T at pressure level p ,

$\tau_1(p)$ = fractional transmittance of the atmospheric CO_2 in channel 1 from pressure level p to $p_0 = .01$ mb,

$x(p)$ = an arbitrary function of pressure which behaves in the vertical similar to $\log p/p_0$.

Term (A) is the atmospheric transmittance of the Planckian radiance from the surface of the earth. Term (B) is the atmospheric contribution to the radiance. Subscripts s and o refer to surface of the earth (1000 mb) and top of the atmosphere (.01 mb), respectively.

When 100 pressure levels are linearly scaled by $p^{2/7}$ and the result adopted for $x(p)$, it follows that

$$p(J) = .01[1 + (J-1)(0.26087836)]^{7/2} \quad (4)$$

and $J = 1,2,\dots,100$ are pressure levels numbered from top of the atmosphere to surface of the earth, the radiative transfer equation can be rewritten [Martin, 1973]

$$I_1 = B_1[T(100)]\tau_1(100) + \int_{J=100}^{J=01} B_1[T(J)] \frac{d\tau_1(J)}{dJ} dJ \quad (5)$$

The Planck radiance function is defined as

$$B_1[T(J)] = c_1 v_1^3 / [e^{(c_2 v_1 / T(J))} - 1] \quad (6)$$

where

$$\begin{aligned} \nu_1 &= \text{wave number for channel 1,} \\ C_1 &= 1.9061 \times 10^{-5} \text{ erg cm}^2 \text{ sec}^{-1} \text{ ster}^{-1}, \\ C_2 &= 1.43868 \text{ cm } ^\circ\text{K.} \end{aligned}$$

When the 100 pressure levels are combined into the 17 atmospheric layers depicted in Fig. 5, eq. (5) can be evaluated in quadrature form

$$I_1 = B_1[T(100)]\tau_1(100) + \sum_{K=1}^{17} \overline{B}_1(K)\Delta\tau_1(K) \quad (7)$$

where

$$\overline{B}_1(1) = \frac{1}{6} \{B_1[T(01)] + 4B_1[T(02.5)] + B_1[T(04)]\} \quad (8)$$

is the layer mean Planck function for layer $K = 1$, and

$$\overline{B}_1(K) = \frac{1}{6} \{B_1[T(J_K-3)] + 4B_1[T(J_K)] + B_1[T(J_K+3)]\} \quad (9)$$

is the layer-mean Planck function for layer $K > 1$. In (7), $\Delta\tau_1(K)$ is the transmittance in channel 1 from layer K as defined by

$$\Delta\tau_1(K) = \tau_1(J_K-3) - \tau_1(J_K+3). \quad (10)$$

Finally, J_K is the value of J at the center of layer K .

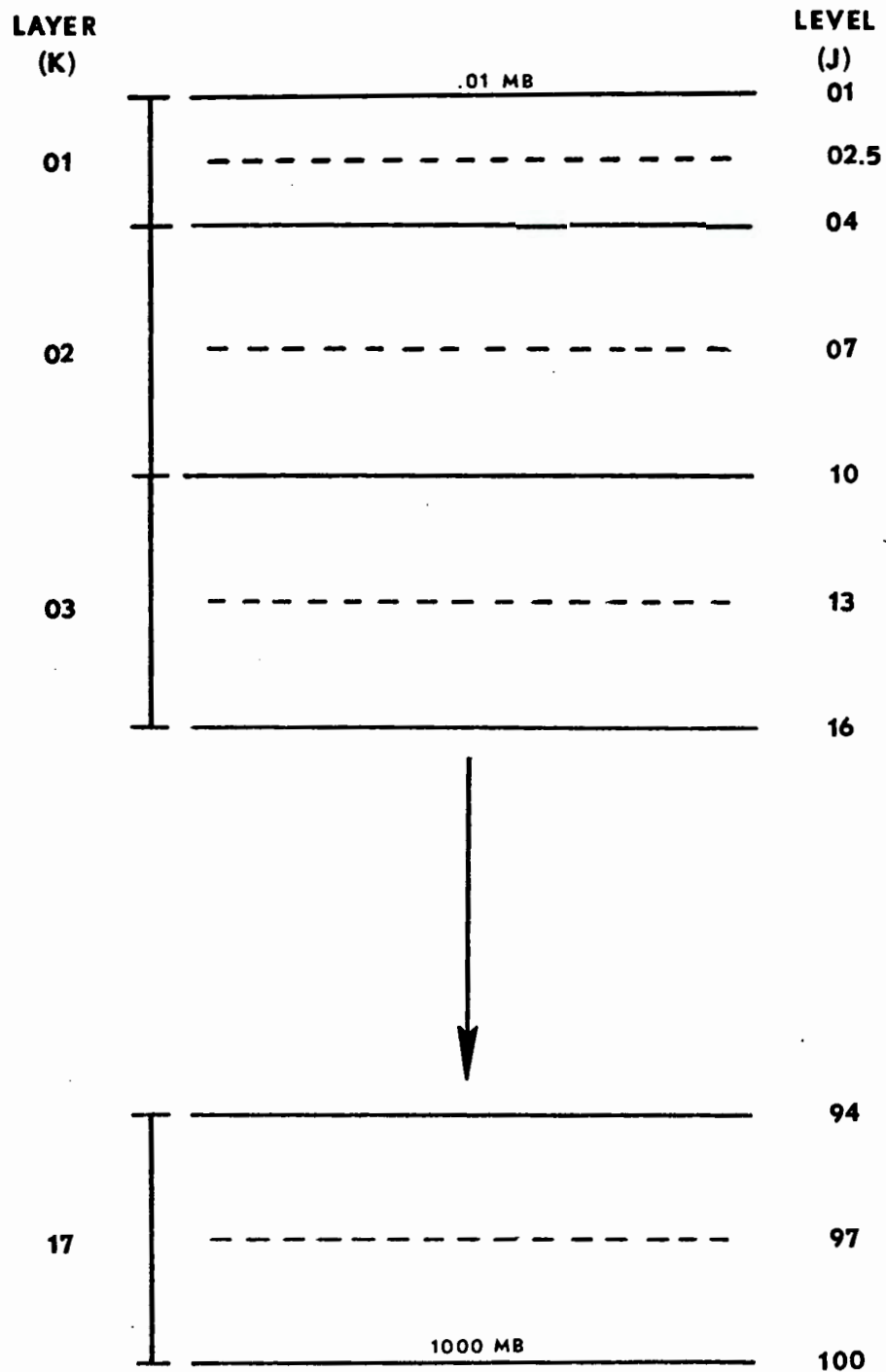


FIG. 5. Seventeen K-layer atmosphere model used for mean-temperature retrieval. Note that the top layer spans only four J-levels while all others span seven J-levels.

Equation (7) can be written in iterative form as

$$I_1 - I_1^n = \{B_1^{n+1}[T(100)] - B_1^n[T(100)]\}\tau_1(100) + \sum_{K=1}^{17} \{\bar{B}_1^{n+1}(K) - \bar{B}_1^n(K)\}\Delta\tau_1(K) \quad (11)$$

where

I_1 = observed radiance for channel 1, considered to be the final iterative value,

I_1^n = calculated radiance for channel 1 from eq. (7) at iteration number n.

Then, following Smith [1970], in each channel the difference

$$\{\bar{B}_1^{n+1}(K) - \bar{B}_1^n(K)\} \quad (12)$$

is independent of pressure within all atmospheric layers; hence the following iterative equation is obtained from eq. (11):

$$\bar{B}_1^{n+1}(K) = \bar{B}_1^n(K) + [I_1 - I_1^n] \quad (13)$$

From a first guess temperature profile $T(J)$, $J = 1, 2, 2.5, 3, \dots, 100$, Planck radiance values, $B_1[T(J)]$ for all channels at each level can be computed from eq. (6). These values can then be used to determine layer mean Planck values, $\bar{B}_1^{(1)}(K)$, by eqs. (8) and (9), and subsequently radiances, I_1 , in accordance with eq. (7). The difference

between observed and calculated radiances, $[I_i - I_i^{(1)}]$, can be applied as a residual correction to obtain adjusted layer mean Planck values, $\bar{B}_i^{(2)}(K)$, by use of eq. (13), and then improved radiances, $I_i^{(2)}$, can be calculated from eq. (7).

By continuing the process of adjusting layer mean Planck values and calculating new radiance values until the difference between observed and calculated radiance for each channel satisfies a convergence criterion at the final iteration step N , final layer mean Planck values, $\bar{B}_i^N(K)$, are obtained for all channels, $i = 1, \dots, 6$ and all layers $K = 1, 2, \dots, 17$.

From the final layer mean Planck values a single mean temperature for each layer can be computed by noting that the fraction of calculated radiance for channel i and layer K , $\Delta I_i(K)$, can be expressed

$$\Delta I_i^N(K) = \bar{B}_i^N(K) \Delta \tau_i(K) \quad . \quad (14)$$

A similar expression applies to each of the six channels for a given layer, and a weighted layer mean Planck value can be formed by summing the $\Delta I_i^N(K)$ over all $i = 1, \dots, 6$. Therefore, for a layer K the weighted layer mean Planck value, $\bar{B}_{w+d}^N(K)$, corresponding to a reference wave number, $\tilde{\nu}_K$, for the layer is computed [Martin, 1973]:

$$\bar{B}_{w+d}^N(K) = \frac{\sum_{i=1}^6 \bar{B}_i^N(K) \Delta \tau_i(K)}{\sum_{i=1}^6 \Delta \tau_i(K)} \quad (15)$$

Substituting the weighted layer mean Planck value into the Planck equation yields

$$\bar{B}_{w+d}^N(K) = c_1 \tilde{\nu}_K^3 / [e^{(c_2 \tilde{\nu}_K / T(K))} - 1] \quad (16)$$

where $\tilde{\nu}_K$ is the reference wave number and $T(K)$ is the mean temperature for layer K at the first guess step of iteration.

The reference wave number for a layer K can be determined by evaluating the weighted layer mean Planck value from eq. (16) using the initial layer mean Planck values $B_1^{(1)}(K)$, substituting the value of $\bar{B}_{w+d}^{(1)}(K)$ thus obtained into a rearranged form of (16)

$$\bar{B}_{w+d}^{(1)}(K) [e^{(c_2 \tilde{\nu}_K / T(K))} - 1] - c_1 \tilde{\nu}_K^3 = 0, \quad (17)$$

and solving for $\tilde{\nu}_K$ using the Bailey iteration method of solution of transcendental differential equations [McCalla, 1967]. Repetition for each layer gives reference wave numbers for all layers, $\tilde{\nu}_K$, $K = 1, 2, \dots, 17$.

The layer mean temperatures for each layer can then be calculated from the weighted layer mean Planck value corresponding to the final layer mean Planck value, $\bar{B}_1^N(K)$, by

$$T(K) = c_2 \tilde{\nu}_K / \ln \left[\frac{c_1 \tilde{\nu}_K^3 + \bar{B}_{w+d}^N(K)}{\bar{B}_{w+d}^N(K)} \right] \quad (18)$$

where $\tilde{\nu}_K$ is the reference wave number computed only at the initial step in accordance with (17).

Layer-mean temperatures may then be converted to layer-thickness values by integrating the hydrostatic equation between top and bottom pressure levels of the layer to obtain the hypsometric equation [Haltiner and Martin, 1957]

$$\Delta Z = \frac{R_d}{g} \bar{T}(K) \ln\left(\frac{p_1}{p_2}\right) \quad (19)$$

where

ΔZ = thickness of a layer in meters,

R_d = 0.287 joules/(gm °K),

g = 9.80 m/sec²,

$\bar{T}(K)$ = mean temperature of the layer in °K,

p_1, p_2 = pressures at top and bottom of layer in mb.

B. APPLICATION

1. Retrieval Input Parameters

In addition to the satellite radiance data already discussed in Section III, first guess temperature profiles for each scan spot and atmospheric transmittance values for all six channels are required as input parameters for the retrieval program.

a. First Guess Temperature Profiles

A first guess temperature profile for each scan spot was derived from 56-level climatological profiles drawn from the U.S. Standard Atmosphere Supplement [1966]. The 15 N annual profile was assumed to be representative of an April profile at that latitude. Profiles for 30 N and

45 N for both January and July were interpolated with respect to time to give equivalent April profiles at each latitude. The three resulting "April" climatological profiles were then expanded to 100 level profiles by interpolating temperature with respect to pressure to give temperatures at the $p^{2/7}$ or J-levels defined by eq. (4).

The 56-level climatological pressure levels and corresponding temperatures for the 15 N as well as the 30 N and 45 N January and July climatological profiles are included in Appendix A, along with the interpolation scheme used for expansion from 56 to 100 level profiles.

Given the latitude of a scan spot, the corresponding first guess profile was obtained by interpolating with respect to latitude only between the 100 level "April" climatological profiles north and south of the scan spot, and by interpolating with respect to pressure between $J = 2$ and $J = 3$ to obtain the $J = 2.5$ level temperature. The 1000 mb climatological temperature was then replaced by the sea-surface temperature to "tie down" the profile at the lower boundary $J = 100$.

b. Atmospheric Transmittance Values

The absorbing gas structure for the six carbon dioxide channels was assumed to be represented by the 100 J-level transmittances listed in Appendix B. These are transmittances calculated for a model atmosphere and the standard temperature profile which is also included in the

Appendix. However, as will be discussed in Section V, some of the transmittance profiles were later adjusted to improve retrieval results.

2. Computational Procedure

In practice, the reduction of VTPR "clear-column" radiances to atmospheric thicknesses was accomplished using two separate computer programs: one to retrieve mean temperatures for all scan spots considered, and a second to convert mean temperatures to thicknesses as well as to sort data by latitude band for analysis by the BIMED 02R regression program. The two programs just described appear with sample outputs immediately following Appendix B.

a. Mean Temperature Retrieval

The procedure for retrieving layer mean temperatures for layers $K = 1, 2, \dots, 17$ from the VTPR "clear column" carbon dioxide radiances can be summarized as follows:

[1] Derive a first guess temperature profile $T(J)$, $J = 1, 2, 2.5, 3, \dots, 100$ in the manner described previously, and compute Planck radiance values, $B_1[T(J)]$, for each J -level using eq. (6).

[2] Calculate layer mean Planck values, $\bar{B}_1^{(1)}(K)$, $K = 1, 2, \dots, 17$ in accordance with eqs. (8) and (9).

[3] Compute reference wave numbers for each layer using the initial layer-mean Planck values to form the weighted layer mean Planck value, $\bar{B}_{\text{wtd}}^{(1)}(K)$ by use of eq. (15) and then solving (17) for $\tilde{\nu}_K$ by the Bailey iterative method.

[4] Use the layer-mean Planck values to calculate the nth iterative radiances, I_1^n , $i = 1, 2, \dots, 6$ by eq. (7).

[5] Compare the observed radiances with the calculated radiances and apply the difference, $[I_1 - I_1^n]$, as a residual correction to adjust the layer-mean Planck values in accordance with (13).

[6] Repeat steps [4] and [5] until convergence is achieved, convergence being defined as that condition in which

$$\left| \frac{[I_1 - I_1^N]}{I_1} \right| < 0.0001 \quad (20)$$

[7] From the final layer-mean Planck values, $\bar{B}_1^N(K)$, compute the corresponding layer-mean temperatures using eq. (18).

b. Standard-layer Thickness Calculation

Instead of calculating thicknesses for the 17 layers for which mean temperatures were retrieved, it was decided to compute thicknesses between standard pressure levels that would permit a more complete and orderly examination of layer combinations for specification of the troposphere and stratosphere as will be discussed in Section VII. The standard pressure levels chosen were the 56-climatological profile levels plus the additional four levels at 650, 550, 450, and 80 mb.

Computation of thicknesses for the larger number of pressure intervals was accomplished by the procedure summarized as follows:

[1] Consider the 17-layer mean temperatures obtained by retrieval to be located at the mid-levels of each layer, that is at levels $J = 2.5, 7, 13, \dots, 97$.

[2] "Tie down" the resulting profile to the sea surface temperature at level $J = 100$ (1000 mb).

[3] Determine the lapse rate between levels $J = 7$ and $J = 2.5$ and continue the lapse rate to level $J = 01$ (.01 mb) to determine the temperature at the top of the atmosphere. This completes a 19-level profile with temperatures at J -levels 1, 2.5, 7, 13, ..., 97, 100.

[4] Interpolate for temperature with respect to pressure, to derive temperatures at the 60 standard pressure levels from the 19-level profile on the J -scale.

[5] Calculate thicknesses of layers between successive standard pressure levels using a modification of the hypsometric equation (19)

$$\Delta Z = \frac{R_d}{g} \frac{(T_1 + T_2)}{2} \ln \left(\frac{p_1}{p_2} \right) \quad (21)$$

where

T_1, T_2 = temperatures ($^{\circ}\text{K}$) at top and bottom pressure levels of the layer under consideration.

IV. EVALUATION OF RETRIEVAL ACCURACY

If matching radiosonde soundings had been available, the retrieved mean temperatures for a given "clear-column" scan spot could have been compared to mean temperatures calculated from the corresponding radiosonde profile. However, matched radiosonde data were not available.

Therefore to evaluate accuracy of the retrieved mean temperatures, profiles constructed from the retrieved temperatures were first compared with the climatologically derived first-guess profiles to determine whether or not there were systematic differences between the two. Next, lapse rates between the bottom and top of layers of thickness $\Delta J = 3$ were examined and layers having super-adiabatic lapse rates were identified.

Retrieved profiles were constructed by assigning mean temperatures to pressure levels at the middle of each layer by extending the lapse rate between levels $J = 7$ and $J = 2.5$ to level $J = 1$ to compute a temperature for the top of the atmosphere, and by "tying down" the profiles by setting the temperature at $J = 100$ equal to the sea surface temperature. With temperatures then fixed for the 19 levels $J = 1, 2.5, 7, 13, \dots, 97, 100$, the temperatures at convenient intermediate levels were computed by interpolation to give the profiles $T(J)$, $J = 1, 2.5, 4, 7, \dots, 94, 97, 100$, defined now at 3^4 J-levels for each scan spot.

Initial retrieval attempts resulted in profiles that were systematically colder than first guess profiles by a few degrees at all levels except $J = 100$ where the retrieval temperature was set equal to the sea surface temperature. The important bias upon retrieval was that super-adiabatic lapse rates of from 12 to 18 °K per km were observed between 1000 and 900 mbs in virtually every retrieved temperature profile. Lapse rates above 900 mbs were approximately the same as those of the profiles derived from climatological standards.

Similar systematic temperature errors were observed in retrieval methods using SIRS-A data [Fritz, Wark, et al., 1972] and VTPR data [Jastrow and Halem, 1973]. In both references, the errors were compensated for by adjusting, or "tuning", the transmittance values channel by channel until the differences between retrieved profiles and the verifying radiosonde profiles at island stations used as check-profiles were brought within acceptable limits. However in this study, without radiosondes to use as check-profiles it was not possible to attempt "tuning" in a sophisticated manner.

Nevertheless, to maintain quality control in the retrieved profiles it was necessary to eliminate the super-adiabatic lapse rates between 1000 and 900 mbs. This could have been done more elegantly, however reducing transmittance values for channel five by a factor of .95 and values for channel six by a factor of .90 proved to be

sufficient for the present purpose. Typical examples of retrieved profiles before and after the "tuning" of the transmittances as just described are depicted in Figs. 6 and 7. Note that the super-adiabatic lapse rates between 1000 and 900 mbs have been corrected by the "tuning" process which will be discussed further in Section V.

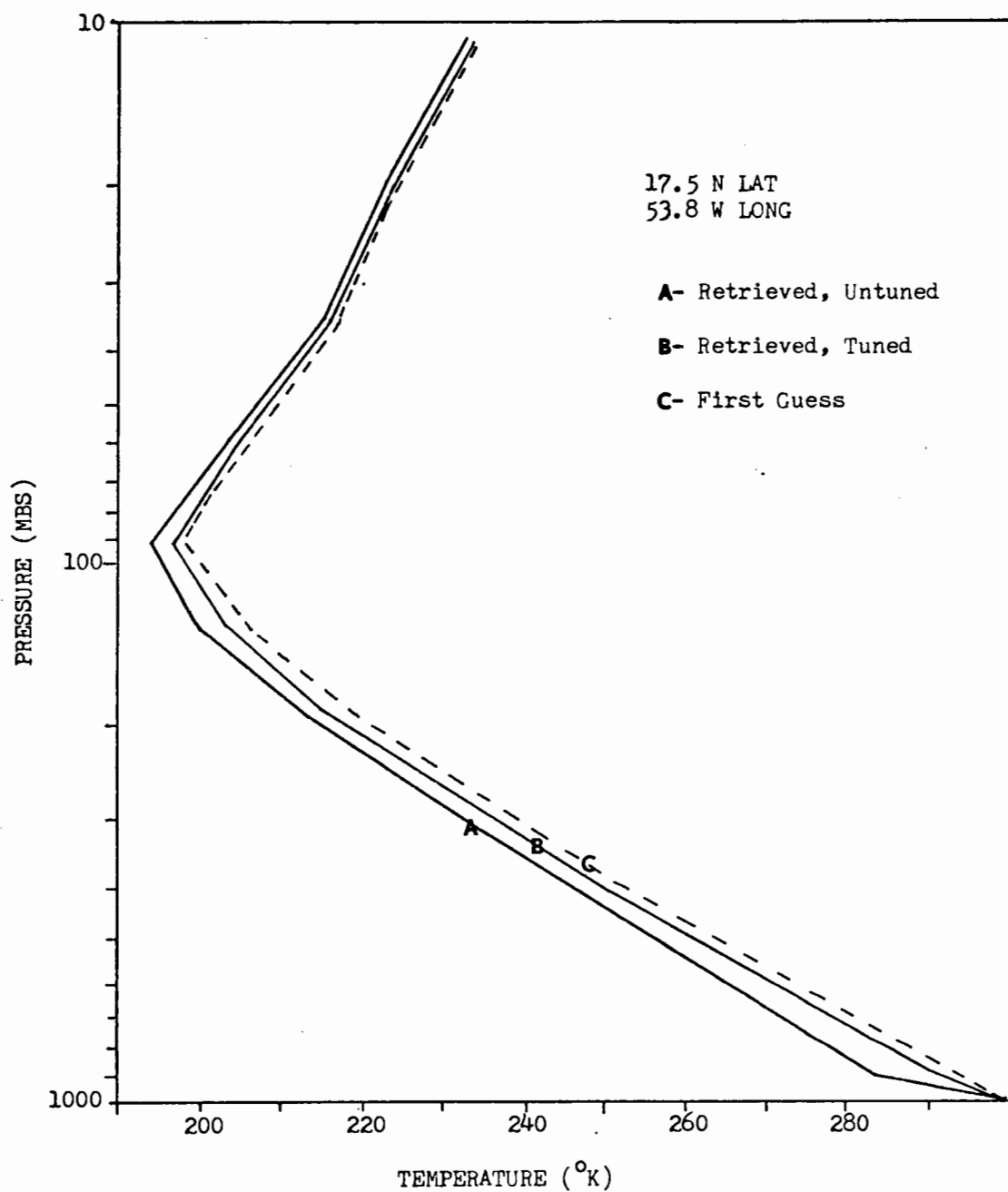


FIG. 6. Low-latitude temperature retrievals using both untuned and tuned transmittances. Note elimination of super-adiabatic lapse rate in lowest 100 mb by the tuned transmittances.

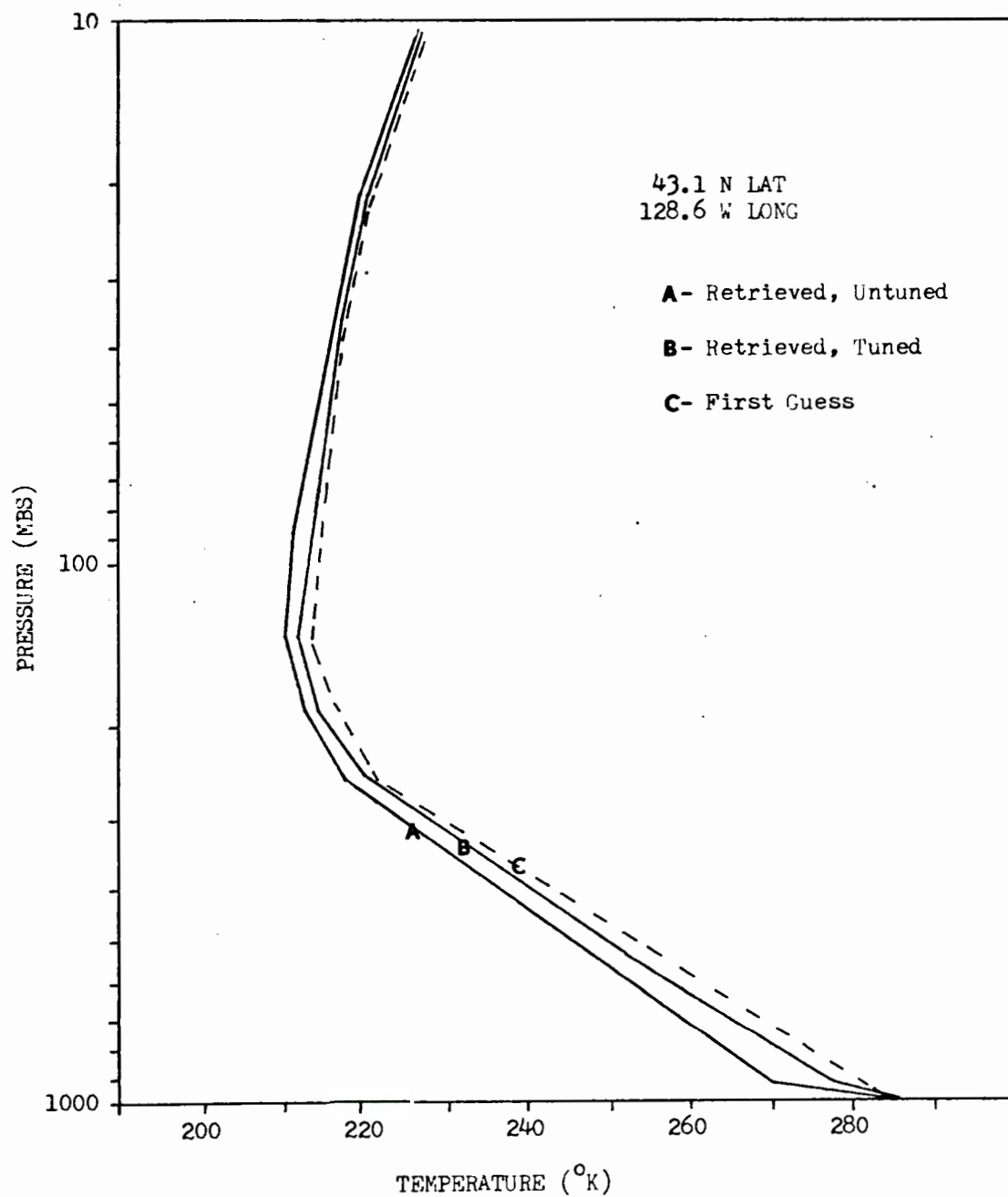


FIG. 7. Mid-latitude temperature retrievals using both untuned and tuned transmittances. Note elimination of super-adiabatic lapse rate in lowest 100 mb by the tuned transmittances.

V. TRANSMITTANCE TUNING

Although there are other possible causes of systematic error in radiance retrieval results, such as improper instrument calibration, the largest single source of such errors is presumably due to uncertainties in the transmittance functions [Drayson, 1971].

Transmittances are computed from theoretical models of absorption band structure, and are uncertain by at least a few percent in each channel [Jastrow and Halem, 1973]. In the case of transmittance functions for the 15 μm carbon dioxide channels, much of this uncertainty is due to lack of precise knowledge of the intensities, half-widths, and shapes of the absorption lines of all molecular absorbers contributing to $\tau_1(p)$. Such knowledge should also be available for the 14 μm band of ozone, and for the 20 μm pure rotational band of water vapor [Drayson, 1971]. The ozone band absorbs weakly in the upper stratosphere, while a weakly absorbing edge of the water vapor band is effective in the lower troposphere.

In addition, the transmittance functions are known to be weakly temperature dependent. For a given standard temperature profile the total transmittance of the atmosphere for VTPR carbon dioxide channels can be considered to be the product of the individual transmittance of carbon dioxide, ozone, and water vapor [McMillin, Wark, et al., 1973]:

$$\tau(p) = \tau_{\text{CO}_2}(p) \cdot \tau_{\text{O}_3}(p) \cdot \tau_{\text{H}_2\text{O}}(p) \quad (22)$$

Since the transmittance values used in this study were carbon dioxide transmittances for a mid-latitude standard atmosphere profile and not subjected to the correction of (22), it was assumed that the standard listings of $\tau(p)$ were not completely descriptive of the absorption profile for the real atmosphere on the day the VTPR measurements were made. These factors are justification for periodic tuning in general [Jastrow and Halem, 1973], and in particular were considered to be the source of the systematic negative temperature errors in the initial retrieved profiles already discussed. Based on this assumption, the transmittances were "tuned" to correct the super-adiabatic temperature lapse rates between 1000 and 900 mbs.

Since the atmosphere transmits more strongly in certain pressure intervals than others for a given channel, the temperature of a given layer can be adjusted by tuning the transmittances for channels which receive greater radiance contributions from the layer. The selective transmittance of the atmosphere is illustrated in Fig. 8 for the "untuned" transmittances. It is clear from the figure that in the layer 1000 to 900 mb the largest atmospheric transmittance is in channels five and six.

From the quadrature form of the radiative transfer equation (7), for a given channel radiance value, I_1 , it follows that selectively decreasing the layer weighting values, $\Delta\tau_1(K)$ requires that the value of the layer mean Planck values, $\bar{B}_1^N(K)$, be increased. An increase in the

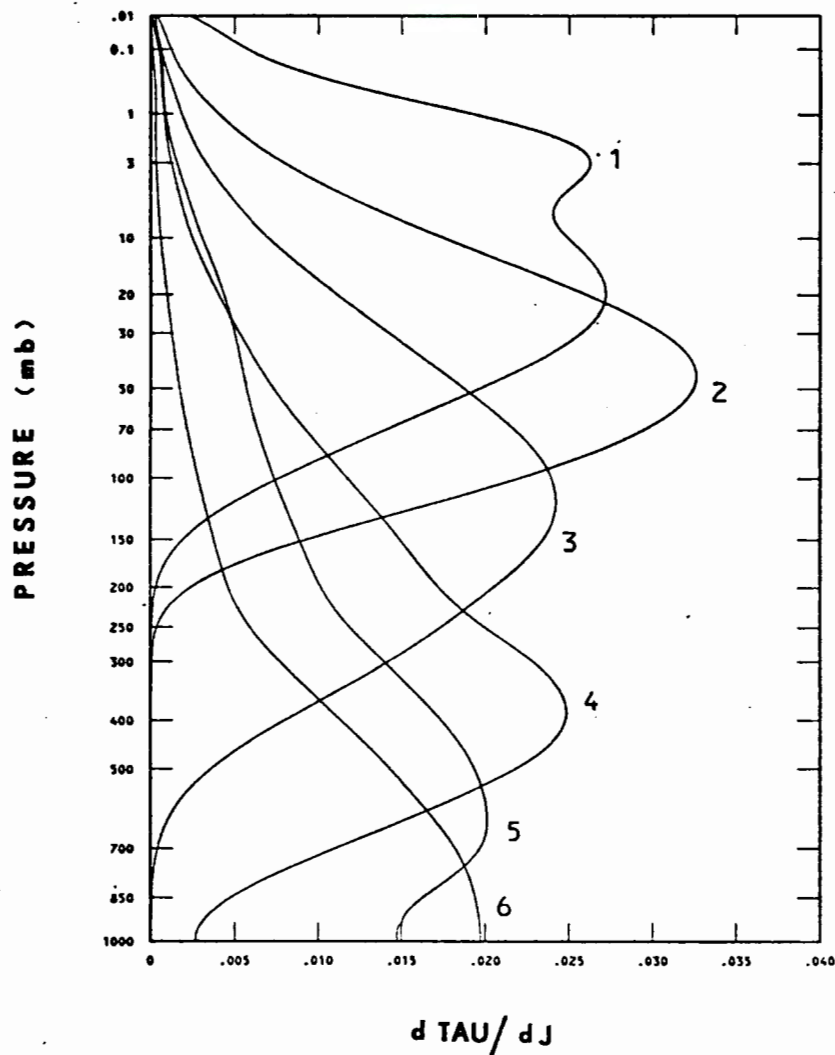


FIG. 8. Weighting functions for VTPR carbon dioxide channels.

layer-mean Planck value will give a higher value for the weighted layer mean Planck for a specific layer evaluated by eq. (15), and that in turn will give a higher layer-mean temperature in accordance with eq. (18).

Increasing the retrieved mean temperature for any layer, K , could therefore be accomplished by decreasing the $\Delta\tau_i(K)$ for channels receiving radiance contributions from the layer.

Since channels five and six most significantly affected the layer 1000 to 900 mbs (as indicated in Fig. 8), increasing the retrieved temperature of this layer by decreasing $\Delta\tau_5(K)$ and $\Delta\tau_6(K)$ was feasible.

Rather than decrease transmittance values for channels five and six only in the lowermost layers, a constant fractional decrease of transmittances was applied at all J-levels thereby decreasing $\Delta\tau_5(K)$ and $\Delta\tau_6(K)$ for all layers, K. Decreasing the transmittances only in the lowermost layers would have increased the temperature of the layer 1000 to 900 mbs, but it also would have had the effect of changing the shape of the $\frac{d\tau(J)}{dJ}$ weighting functions for channels five and six. Since a main objective of this thesis was to determine which atmospheric layer thicknesses were best specified by the VTPR "clear column" radiances, a tuning method which did not change the layers in which the $\frac{d\tau(J)}{dJ}$ curves "peaked" was considered desirable, in the absence of radiosonde check-profiles to justify more complex tuning. The fractional decrease of transmittances at all levels satisfied this condition and had the effect of shifting the $\frac{d\tau(J)}{dJ}$ curves of Fig. 8 for channels five and six slightly to the left while retaining their original shape.

The selection of transmittance tuning factors, .95 for channel five and .90 for channel six, was strictly empirical. However subsequent to completion of the retrieval computations, it was learned through private communication [Dr. L. M. McMillin, 1973] that NESS had made somewhat similar tuning adjustments for these two channels for the same VTPR data analysis.

VI. RETRIEVED THICKNESS ANALYSIS

A. INDIVIDUAL LAYER SPECIFICATION

Individual layer thicknesses were subjected to stepwise multiple regression analysis to determine which particular atmospheric layer thicknesses were best specified by using the "clear-column" radiance measurements as predictors.

Prior to statistical analysis, retrieved thicknesses were separated into three samples based on the latitudes of their corresponding VTPR scan spots. Latitude bands and number of scan spots for which thicknesses were retrieved are listed in Table 2.

TABLE 2. Scan spot samples for statistical analysis of retrieved thickness values.

Latitude Band	Latitude of Scan Spots	Sample Size
1	15 N \leq Lat < 25 N	82
2	25 N \leq Lat < 35 N	104
3	35 N \leq Lat < 45 N	109

1. Stepwise Regression Analysis

The Stepwise Regression Analysis Program BIMED 02R [Dixon, 1966] was used to analyze thickness data from the three latitude band samples.

BIMED 02R computes, in a stepwise manner, a sequence of linear regression equations, with one variable added to the regression equation at each step. The variable added is the one that results in the greatest reduction in the previously unexplained sum of squares. This is also the variable which has the highest partial correlation with the dependent variable at the particular step in the analysis of variance. In addition, it is the variable which would have the highest F_k -value when added at step k.

The F_k -value at each step k is [Crow, et al., 1955]

$$F_k(1, n-k-1) = \frac{\%(C.E.V.k) - \%(C.E.V.k-1)}{\%(U.E.V.k)} \quad (24)$$

where

$\%(C.E.V.k)$ is the percent cumulative explained variance at step k.

$\%(C.E.V.k-1)$ is the percent cumulative explained variance, step k-1.

$\%(U.E.V.k)$ is the percent unexplained variance at step k.

This study employed a statistical model expressed as

$$\Delta z = C_0 + C_1 N_1 + C_2 N_2 + C_3 N_3 + C_4 N_4 + C_5 N_5 + C_6 N_6 + C_7 N_7 \quad (25)$$

where Δz is a standard layer thickness, N_1 through N_6 are radiance predictors corresponding to VTPR "clear-column" radiance measurements of channels one through six, and

N_7 is that computed for the window channel (channel eight) from the sea surface temperature by assuming a transmittance of unity [McMillin, Wark, et al., 1973]. C_0 through C_7 are regression coefficients computed by BIMED 02R.

For examination of the troposphere, the dependent variables, or predictands, were all possible layer thicknesses between the pressure levels considered from 1000 to 100 mb. For examination of the lower stratosphere, predictands were all possible layer thicknesses from 100 to 20 mb. Each dependent variable was subjected to the BIMED 02R stepwise multiple regression analysis to determine how well the layer thickness was specified by the independent variables, the "clear-column" radiances.

Related statistical parameters from the BIMED 02R output included:

- a. multiple R
- b. standard error of estimate, S.E.
- c. mean value, $\overline{\Delta z}$
- d. standard deviation, σ
- e. F_k -value
- f. R^2

The most significant parameters for purposes of this study were R^2 and S.E., which are related as follows:

$$(S.E.)^2 = \sigma^2[(n-1)/(n-k-1)](1-R^2) \quad (26)$$

where

$$\sigma^2 = \frac{n}{\sum_{i=1}^n} (\Delta z_i - \overline{\Delta z})^2 / (n-1) \quad (27)$$

is the variance of a layer thickness for the sample, and

n = sample size

i = sample-element identifier

k = number of predictors selected ($k = 7$ in this study).

The fractional unexplained variance $(1 - R^2)$, can be approximated by

$$(1 - R^2) \approx \left(\frac{S.E.}{\sigma} \right)^2 \quad (28)$$

since $(n - k - 1)/(n - 1)$ is close to unity for the sample sizes and number of predictors considered.

The fractional explained variance can then be expressed

$$R^2 = 1 - \left(\frac{S.E.}{\sigma} \right)^2 \quad (29)$$

which becomes the percent explained variance upon multiplying R^2 by 100.

The greater the percent explained variance for a particular layer thickness, the better the thickness is considered to be specified by the radiance predictors.

2. Individual Layer Results

Although the specification of individual layers varied somewhat from latitude band to latitude band, in

general, the layer thicknesses best specified by the VTPR "clear-column" radiances were for relatively large pressure intervals, where also the lower pressure level was in the lower troposphere. Layer thicknesses most poorly specified were for pressure intervals in vicinity of the tropopause.

A total of 99 different layer thicknesses were examined between 1000 and 20 mb for each latitude band. Rather than tabulate the statistical parameters for all 99 layers, a representative group of layer thickness results has been extracted which illustrates the general trends in thickness specifications.

Statistical parameters for a set of sequential layers between 1000 and 20 mb for all three latitude bands are listed in Table 3. Note that layers in vicinity of the tropopause, that is those between 150 and 90 mb, were not as well specified in terms of fractional explained variance as the layers above and below. This is indicative of "noise" in the retrieved mean temperatures near the tropopause associated with the reversal of temperature gradient across the interface. Both Tables 3 and 4 show that the explained variance of the thickness of layers in vicinity of the tropopause (e.g. 150-100, 100-90 mb) increases with increased latitude. Statistically this was a result of the larger standard deviations in the thicknesses of layers 150 to 100 mb and 100 to 90 mb as one progresses into mid-latitude bands. Give a larger σ^2 , the variable Δz is more predictable in terms of layer-mean temperature and/or radiances.

TABLE 3. Statistical parameters of some representative sequential layers.

Pressure Layer (mb)	Band 1		Band 2		Band 3	
	S.E. (gpm)	R ²	S.E. (gpm)	R ²	S.E. (gpm)	R ²
30-20	1.670	.9779	1.487	.9856	1.661	.9865
50-30	2.123	.9810	2.981	.9693	2.940	.9758
70-50	6.175	.8110	5.731	.8622	5.474	.8982
90-70	7.966	.6627	6.222	.8083	5.650	.8662
100-90	3.792	.6052	2.914	.7847	2.623	.8559
150-100	9.352	.6076	8.907	.7487	8.558	.8622
200-150	1.594	.9317	3.686	.8021	3.752	.9283
250-200	0.489	.9944	0.844	.9876	0.802	.9954
300-250	0.748	.9863	0.514	.9956	0.532	.9978
400-300	1.572	.9803	1.436	.9897	1.504	.9945
500-400	1.255	.9821	1.469	.9853	1.531	.9921
600-500	0.957	.9861	1.415	.9816	1.487	.9901
700-600	2.532	.9777	1.403	.9769	1.467	.9877
1000-700	2.532	.9797	2.929	.9813	2.960	.9894

TABLE 4. Statistical parameters of some layers of special interest

Pressure Layer (mb)	Band 1		Band 2		Band 3	
	S.E. (gpm)	R ²	S.E. (gpm)	R ²	S.E. (gpm)	R ²
300-150	0.384	.9995	4.053	.9638	4.072	.9862
400-150	1.230	.9982	2.826	.9932	2.724	.9974
500-150	2.496	.9957	1.778	.9985	1.594	.9995
600-150	3.452	.9944	1.505	.9993	1.462	.9997
700-150	4.540	.9927	2.338	.9987	2.446	.9994
150-100	9.352	.6076	8.907	.7487	8.558	.8622
200-100	11.006	.6565	12.603	.7383	12.306	.8813
250-100	10.520	.7481	13.319	.7679	13.084	.9105
100-90	3.792	.6052	2.914	.7847	2.623	.8559
100-70	11.704	.6449	9.136	.8008	8.274	.8628
1000-300	7.399	.9808	8.668	.9833	8.939	.9909
1000-150	7.090	.9989	5.011	.9892	5.156	.9982
1000-100	2.390	.9988	4.351	.9972	4.245	.9989
150-20	27.430	.8435	26.164	.8787	24.616	.9144
100-20	17.445	.9024	16.230	.9239	15.0312	.9446

The sequential layers best specified were those between 600 and 200 mb. These layers are below the highly variable tropopause region, and furthermore are in a pressure interval where significant transmittance of radiance in channels three through six occurs (see Fig. 8). Presumably, having significant radiance contributions in a given layer by several VTPR channels improves specification of the layer thickness by the radiance measurements.

Statistical parameters for thicknesses of layers of special interest are listed in Table 4. These include the layers generally best specified, the layers generally most poorly specified, the 1000 to 300 mb layer thickness currently used in the FNWC vertical-analysis scheme [Holl et al., 1964], and the defined "tropospheres" and "stratospheres" to be discussed in Sections VI (B) and (C). As in the case of sequential layers already discussed, the most poorly specified of all pressure intervals in Table 4 were shallow and had boundaries near the tropopause. The best specified layers were those in the mid-troposphere where significant radiance contributions from at least four of the CO₂ channels occur.

B. TROPOSPHERIC SPECIFICATION BY SUB-LAYERS

Results of the statistical regression analysis applied to individual layers were next used to examine various combinations of the sequential sub-layers in the troposphere to determine which of the combinations could best specify the full tropospheric thickness.

1. Method of Analysis

To compare the results of different tropospheric thickness combinations, a normalized root mean square error index was defined. The error index, E.I., for a two-layer combination, for example, was

$$E.I. = \frac{\sqrt{S.E._1^2 + S.E._2^2}}{\bar{\Delta z}_{trop}} \quad (30)$$

where $S.E._1$ and $S.E._2$ are the standard errors of estimate for the individual layers, and $\bar{\Delta z}_{trop}$ is the mean thickness of the defined troposphere. Similarly, the E.I. for a three-layer combination was

$$E.I. = \frac{\sqrt{S.E._1^2 + S.E._2^2 + S.E._3^2}}{\bar{\Delta z}_{trop}} \quad (31)$$

Weighting of standard errors when computing the E.I. for a particular layer combination was not required since the standard error of thickness reflects variance in the retrieved mean temperatures, and weighting of mean temperatures by $\ln(p_1/p_2)$ factors was implicit in conversion of mean temperatures to thicknesses by the hypsometric equation.

This error index expresses combined layer errors in a root mean square (RMS) sense, and the smaller the E.I. value the better the combination of layers specifies the total thickness.

Specification of the tropospheric thickness was considered by defining the troposphere in one series of tests to be the layer 1000 to 100 mb, and in a second series of tests to be the layer 1000 to 150 mb. In each case, best specification of the "troposphere" was sought by comparing error-index values for various sub-layer combinations within the troposphere.

To form combinations of layers, the concept of a "sliding layer" was adopted. The "sliding layer" was first tied down to the 1000 mb level and the RMS error, as expressed by the error index, was computed for the resulting two-layer combination. The sliding layer was then stepped to a higher level and the RMS error for the resulting three-layer combination calculated. The procedure of stepping the sliding layer to higher levels to form new combinations was continued until a final two-layer combination was formed with the top of the sliding layer being coincident with the defined tropopause level (150 or 100 mb). The pressure interval of the sliding layer was then increased and the procedure repeated. "Sliding layers" of 300, 400, 500, 600, 700, and 800 mb were employed. Fig. 9 illustrates the combinations of sub-layers formed by the 400 mb sliding layer in the 1000 to 100 mb troposphere analysis.

Error index values from all combinations of layers formed by the above procedure were compared to determine which particular combination gave the minimum RMS error for specification of the full tropospheric thickness. In

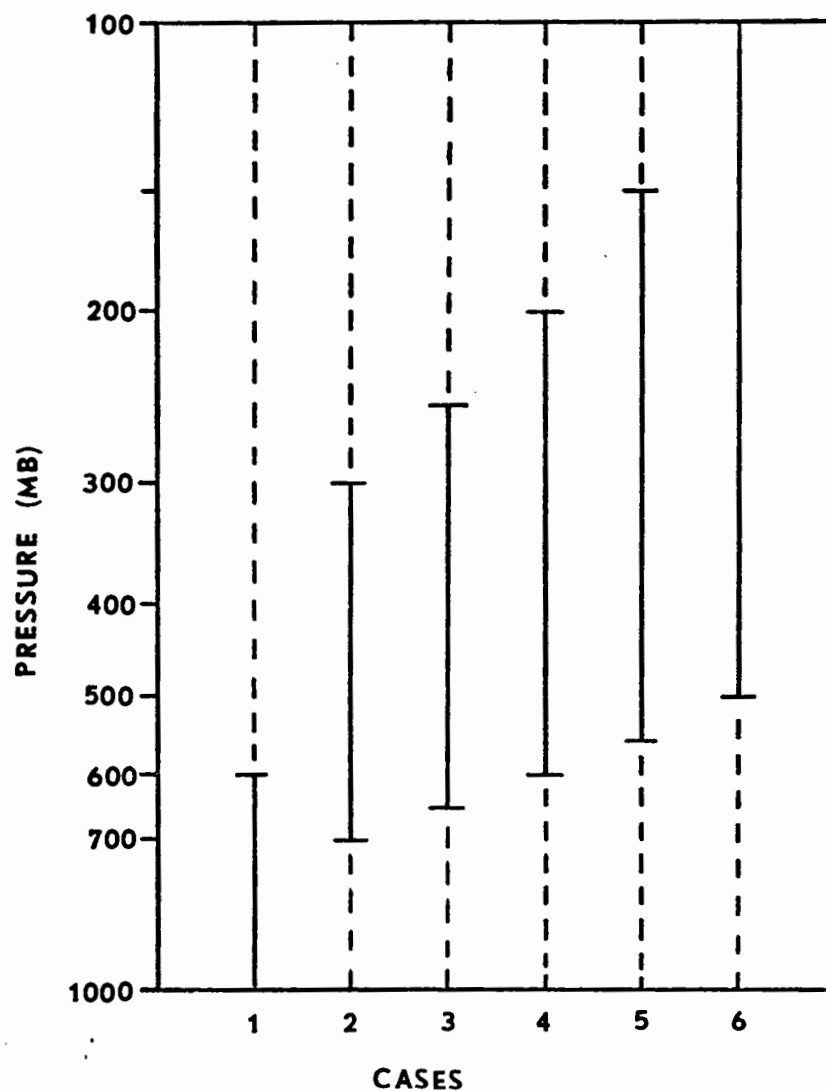


FIG. 9. All combinations, or cases, of tropospheric sub-layers formed by the 400 mb "sliding layer" with the tropopause defined at 100 mb. In each case, the combined sub-layers span the pressure interval 1000-100 mb and the location of the sliding layer is indicated by the solid line.

addition, the combination layer results were compared against the E.I. values for the "tropospheres" considered as single layers, 1000 to 150 mb and 1000 to 100 mb.

2. Troposphere Results

In all three latitude bands, defining the troposphere to be the pressure interval 1000 to 150 mb, rather than 1000 to 100 mb, resulted in generally lower E.I. values for the layer combinations considered. This result can be attributed to the fact that the single layer 150 to 100 mb was the most poorly specified of all troposphere layers due to variability induced by the tropopause in this layer. Therefore defining the model tropopause at 150 mb gave smaller combined error index values by eliminating errors of the 150 to 100 mb layer.

In latitude bands two and three, the maximum RMS error for both two and three layer combinations occurred when the lower limit of the top layer of a combination was at 250 mb. In latitude band one this maximum occurred when the lower limit of the top layer was at 200 mb. This result may also be explained in terms of influence of the tropopause, since the tropopause is generally higher in lower latitudes [Haltiner and Martin, 1957], and therefore its detrimental effect on the standard error of estimation is greater for the layer 200 to 100 mb than for the layer 250 to 100 mb as in the higher latitude bands. Standard error values for these layers listed in Table 4 illustrate this relationship.

The general trend in the troposphere was for the combination error index values to be lowest for certain two-layer combinations topped at 150 mb with a dividing level near 650 mb (Table 5). Table 5 lists in sequence the layer-combinations found here to be most effective in giving minimum error index values. Examination of Figs. 10, 11, 12 show that other layer choices give rise to larger RMS errors of specification in the troposphere. No attempt has been made in this study to ascribe statistical significance to any one layer choice because of the limited period of the test. However, the general nature of the "best" results in each band seem to resemble the tropospheric stratification already described.

When the RMS errors for layer combinations were compared against those for the "tropospheres" taken as single layers, it was found that the layer 1000 to 150 mb could be better specified by certain combinations of sub-layers than when considered as a single layer. The layer 1000 to 100 mb, however, had the minimum of all RMS errors found when considered as a single layer. This evidently was due to the fact that the relatively poor specification in the 150 to 100 mb layer became insignificant in comparison to the thickness-specification of the layer 1000 to 100 mb. Error index values for the two defined troposphere layers considered as single layers are listed by latitude band in Table 6, and these may be compared with the best combination results in Table 5. Note that the best

TABLE 5. Tropospheric sub-layer combinations having the smallest error index values.

Pressure Layers (mb)	Band 1	E.I.
1000-700, 700-400, 400-150		.000315
1000-700, 700-100		.000341
1000-550, 550-150		.000370
	Band 2	
1000-700, 700-150		.000275
1000-650, 650-150		.000308
1000-600, 600-150		.000338
	Band 3	
1000-700, 700-150		.000284
1000-650, 650-150		.000316
1000-600, 600-150		.000345

specification of the troposphere in each latitude band was obtained by considering the single alyer 1000 to 100 mb.

TABLE 6. Error index values for the defined "tropospheres" considered as single layers.

"Troposphere" (mb)	Band 1 E.I.	Band 2 E.I.	Band 3 E.I.
1000 to 100	.000148	.000271	.000265
1000 to 150	.000515	.000364	.000382

Error index values for all tropospheric layer combinations considered, as well as values for the defined tropospheres taken as single layers, are graphically depicted in Figs. 10, 11, and 12. For each latitude band, graphs (a), (b), (c) depict E.I. values for layer combinations formed by "sliding layers" of 300, 400, and 500 mb. The (d) graph for each band depicts E.I. values for all other combinations considered, that is combinations resulting from sliding layers of 600, 700, and 800 mb, as well as error index values for the single layer troposphere cases.

Note that except for the two-layer combination 1000 to 700 and 700 to 100 mb in latitude band one, all other combinations formed by sliding layers had smaller error index values when the tropopause was defined at 150 mb. Also note the shift in maximum E.I. value from

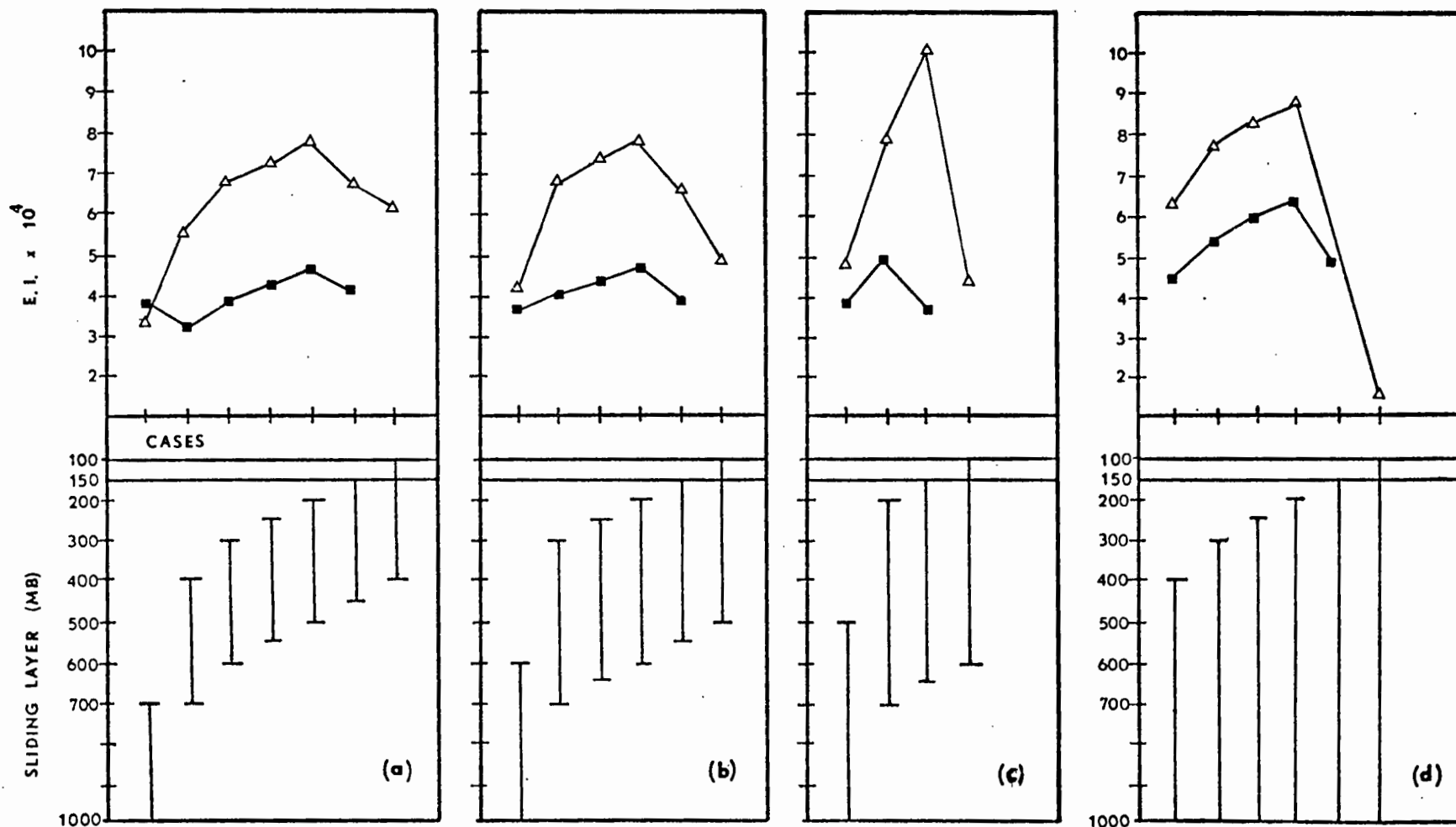


FIG. 10. Cases of tropospheric sub-layer combinations considered and corresponding error index values (15 N to 25 N).

■ E.I. values with tropopause at 150 mb. △ E.I. values with tropopause at 100 mb.
 (a) Sub-layer combinations formed by sliding layer of 300 mb, (b) 400 mb,
 (c) 500 mb, (d) all others.

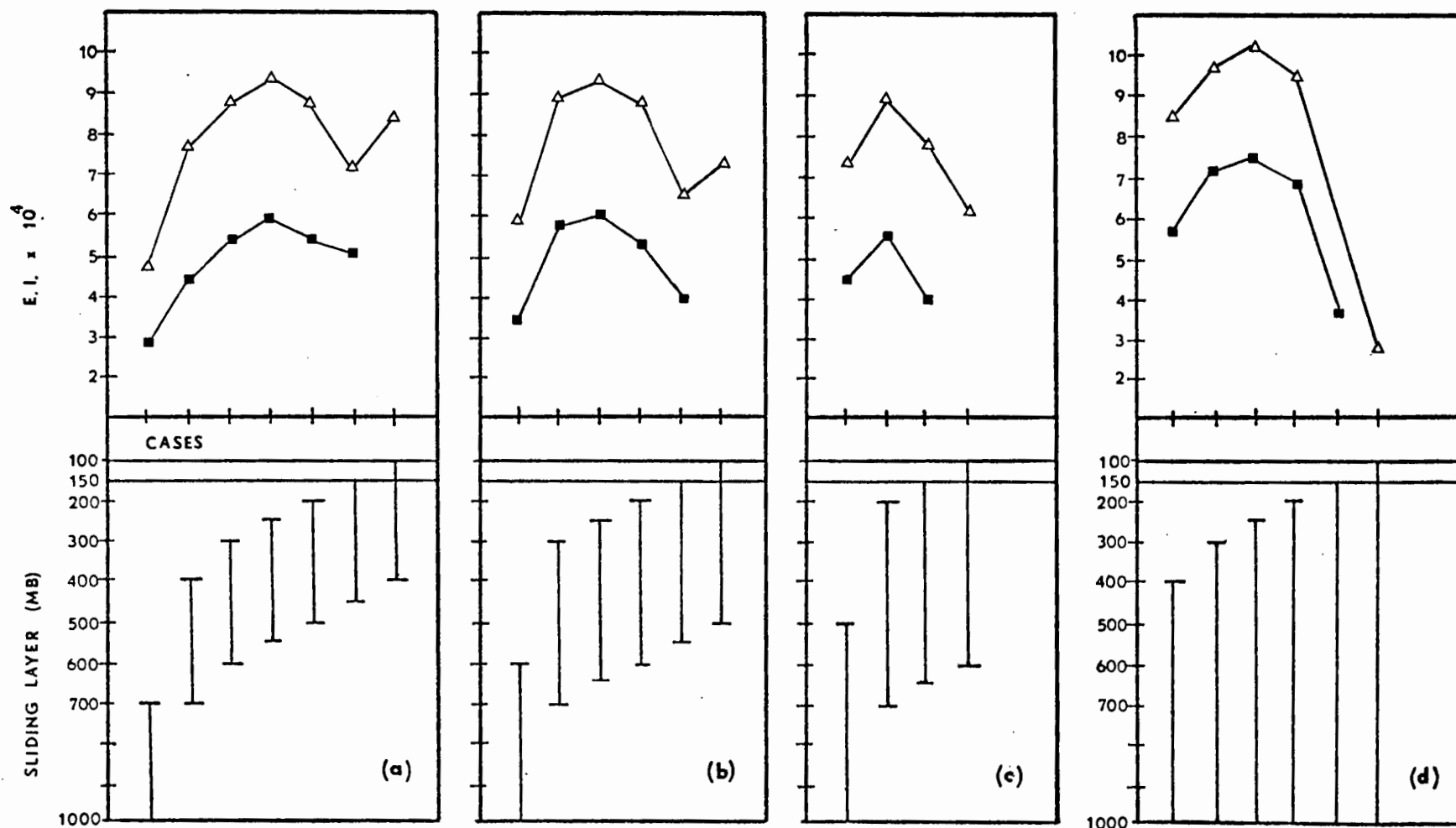


FIG. 11. Cases of tropospheric sub-layer combinations considered and corresponding error index values (25 N to 35 N).

■ E.I. values with tropopause at 150 mb. △ E.I. values with tropopause at 100 mb.
 (a) Sub-layer combinations formed by sliding layer of 300 mb, (b) 400 mb,
 (c) 500 mb, (d) all others.

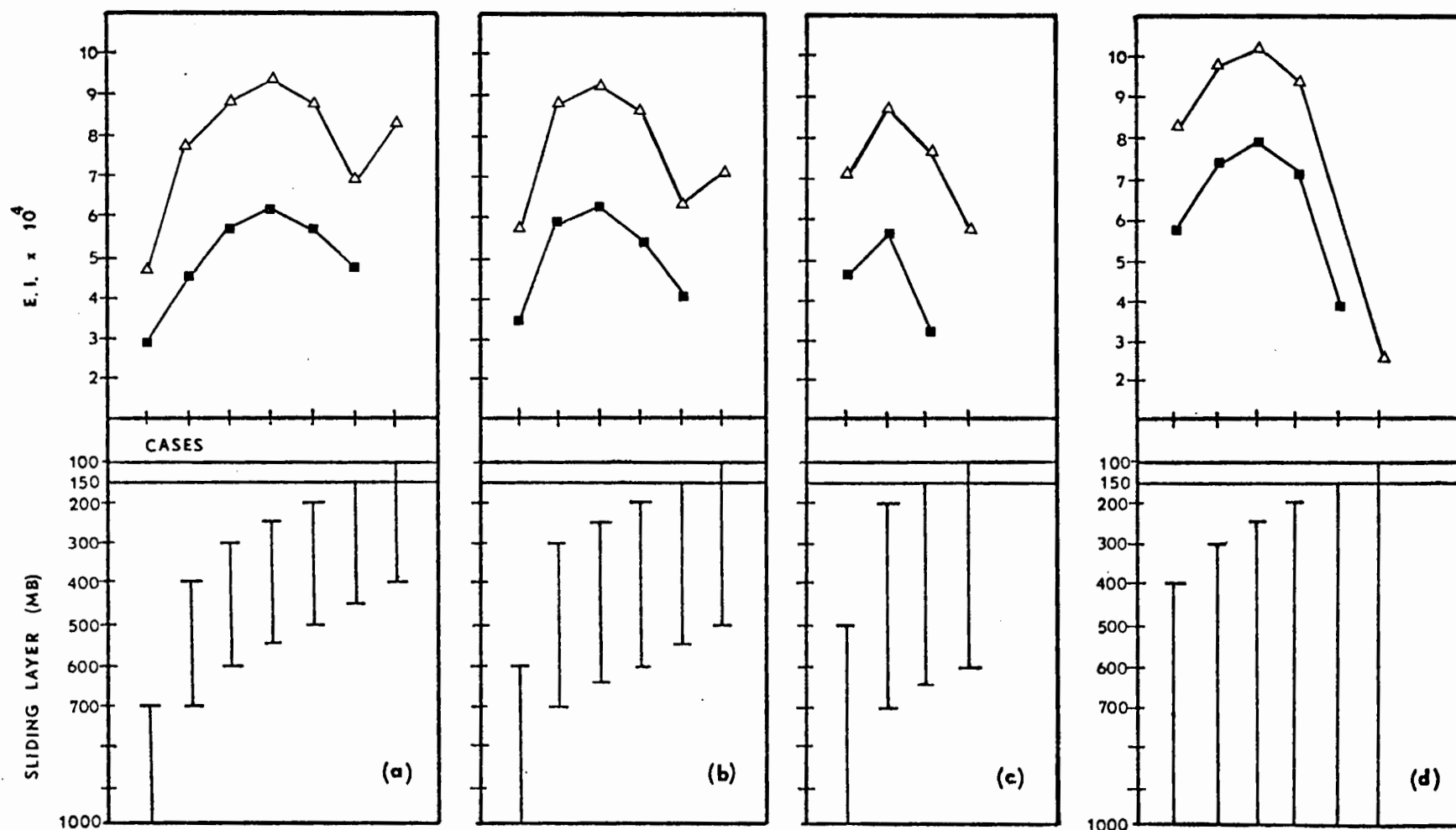


FIG. 12. Cases of tropospheric sub-layer combinations considered and corresponding error index values (35° N to 45° N).

■ E.I. values with tropopause at 150 mb. △ E.I. values with tropopause at 100 mb.
 (a) Sub-layer combinations formed by sliding layer of 300 mb, (b) 400 mb,
 (c) 500 mb, (d) all others

combinations with the topmost layer having a lower limit at 200 mb in band one to combinations with the topmost layer having a lower limit at 250 mb in bands two and three.

C. STRATOSPHERIC SPECIFICATION BY SUB-LAYERS

Best specification of the stratosphere to 20 mb was sought in a manner similar to that of the troposphere already discussed.

1. Method of Analysis

The error index was as defined in specification of the troposphere, except that $\overline{\Delta z}_{\text{strat}}$ was used instead of $\overline{\Delta z}_{\text{trop}}$ in eqs. (30), (31). The stratosphere was considered in one series of tests to be the layer 150 to 20 mb, and in a second series of tests to be the layer 100 to 20 mb. "Sliding layers" of 30, 40, 50, 60, 70, and 80 mb were used to form layer combinations. Figure 13 illustrates the layer combinations formed by the 30 mb sliding layer between 150 and 20 mb.

2. Stratosphere Results

Although the results do not afford as sharp a specification as for the troposphere, a general result was that the 100 to 20 mb "stratosphere" had lower RMS errors for layer combinations than the 150 to 20 mb case. This again can be attributed to the influence of the tropopause in the layer 150 to 100 mb. By defining the tropopause to be at 100 mb the poorer specification of the layer 150 to 100 mb was eliminated.

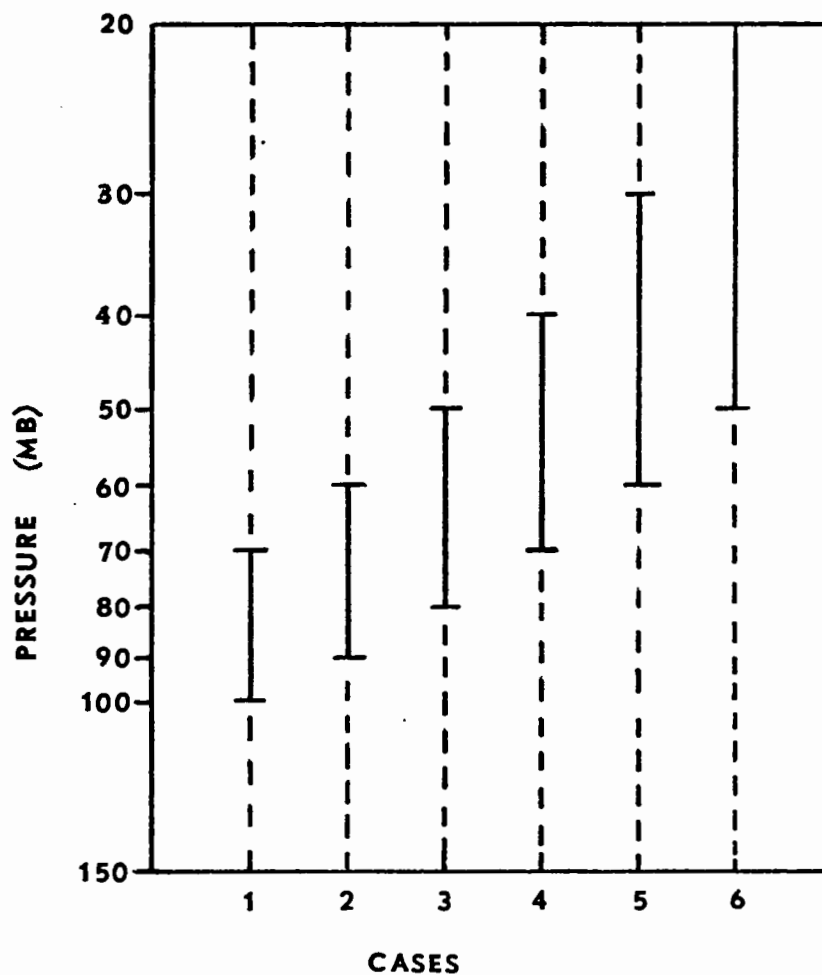


FIG. 13. All combinations, or cases, of stratospheric sub-layers formed by the 30 mb "sliding layer" with the tropopause defined at 150 mb. In each case, the combined sub-layers span the pressure interval 150-20 mb and the location of the sliding layer is indicated by the solid line.

The three best layer combinations in each latitude band are listed sequentially in Table 7 with their corresponding error index values. There was not a unique set of combinations that proved to be most effective for all latitudes, but a general trend for the error index of best combinations to decrease with increasing latitude is evident. This apparently was a result of the tropopause being at lower levels for higher latitudes, which tended to reduce the influence of the tropopause on specification of the defined stratosphere above 100 mb at higher latitudes. As in the tropospheric analysis, no attempt has been made to attach statistical significance to the results due to the limited period of the test.

Error index values for the two "stratospheres" considered as single layers were not as good as for combinations of layers. A decrease in E.I. values when the 150 to 100 mb layer was incorporated into the total thickness was not observed as in the troposphere analysis. This difference was evidently due to the fact that the thickness-error induced by the 150 to 100 mb layer was relatively smaller in comparison to the specification of the full tropospheric thickness, but had greater influence on thickness-error of the stratosphere. Error index values for the two defined stratosphere layers are listed by latitude band in Table 8.

Error index values for all stratospheric layer combinations considered, as well as values for the defined

TABLE 7. Stratospheric sub-layer combinations having the smallest error index values.

Pressure Layers (mb)	Band 1	E.I.
100-90, 90-60, 60-20		.00123
100-80, 80-20		.00130
150-100, 100-70, 70-20		.00131
	Band 2	
100-90, 90-60, 60-20		.00105
100-80, 80-50, 50-20		.00112
100-70, 70-20		.00116
	Band 3	
100-70, 70-30, 30-20		.00094
100-80, 80-40, 40-20		.00095
100-90, 90-60, 60-20		.00096

TABLE 8. Error index values for the defined "stratospheres" considered as single layers.

"Stratosphere" (mb)	Band 1 E.I.	Band 2 E.I.	Band 3 E.I.
100 to 20	.00172	.00162	.00148
150 to 20	.00220	.00214	.00198

stratospheres taken as single layers, are graphically depicted in Figs. 14, 15, and 16. For each latitude band, graphs (a), (b), (c), (d) depict E.I. values for layer combinations formed by 30, 40, 50, and 60 mb "sliding layers"; (e) graph depicts error index values for the single-layer stratosphere cases in addition to those for the 70 and 80 mb sliding layer combinations.

The graphical display of stratospheric error index values illustrates the fact that defining the tropopause to be at 100 mb gave better E.I. values than when the tropopause was defined at 150 mb and the layer 150 to 100 mb was included in the stratospheric specification. Also note that the E.I. values are an order of magnitude greater than the tropospheric error index values previously examined.

Apparently, the significantly greater E.I. values in the stratosphere are due to standard errors of estimate, S.E., of layers in the stratosphere reflecting uncertainties of explained variance for the tropospheric column below, as well as for the layers of the stratosphere. In the

troposphere, on the other hand, the layer combinations are "tied down" to the surface and tropospheric standard errors reflect only unexplained variance in the troposphere. Essentially, the relatively greater S.E. values of the stratosphere result in correspondingly greater E.I. values, although $\overline{\Delta z}$ of the denominator is somewhat smaller than for the tropospheric case.

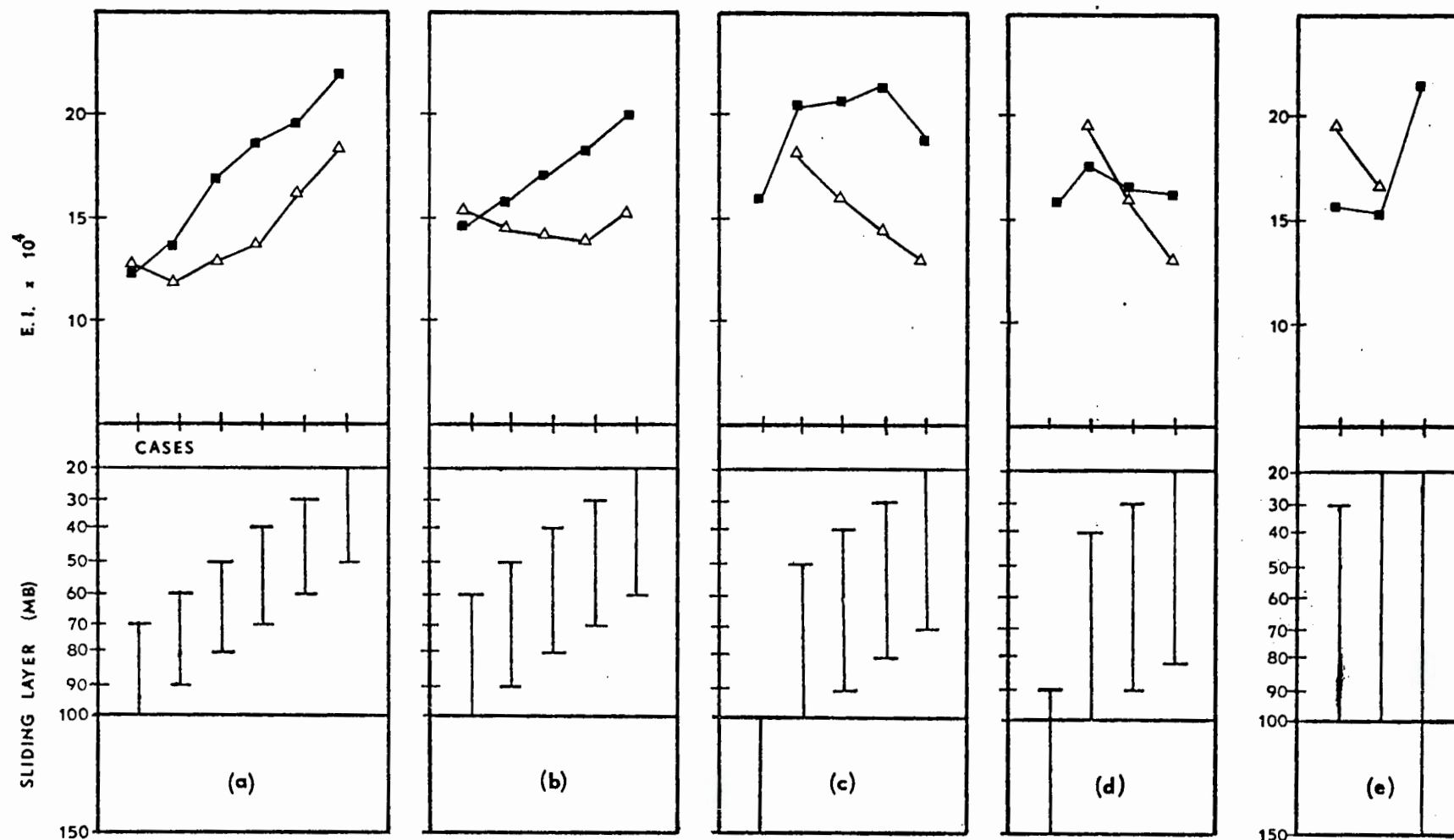


FIG. 14. Cases of stratospheric sub-layer combinations considered and corresponding error index values (15°N to 25°N).

■ E.I. values with tropopause at 150 mb. △ E.I. values with tropopause at 100 mb.
 (a) Sub-layer combinations formed by sliding layer of 30 mb,
 (b) 40 mb, (c) 50 mb, (d) 60 mb, (e) all others.

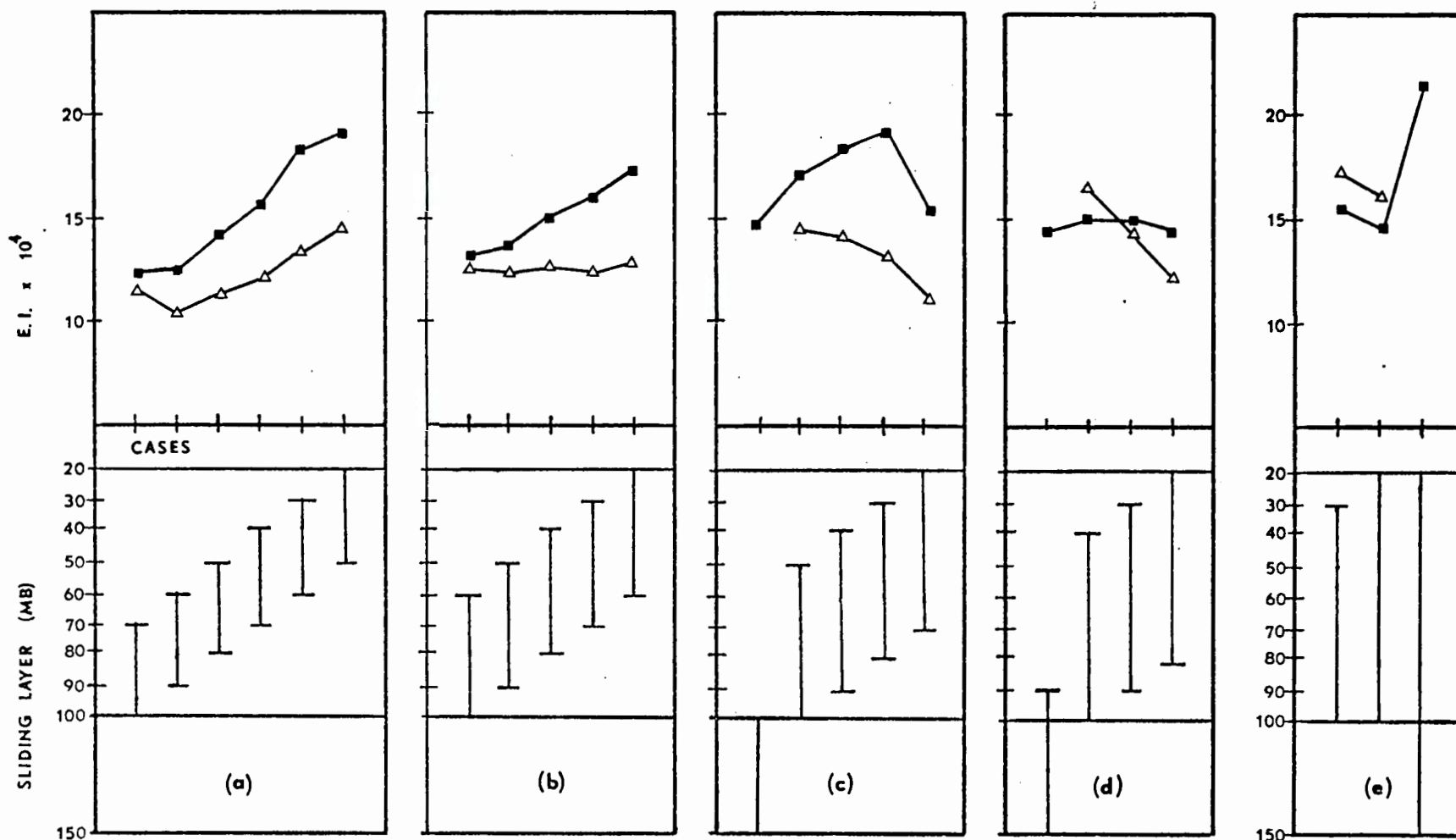


FIG. 15. Cases of stratospheric sub-layer combinations considered and corresponding error index values (25 N to 35 N).

■ E.I. values with tropopause at 150 mb. △ E.I. values with tropopause at 100 mb.
 (a) Sub-layer combinations formed by sliding layer of 30 mb,
 (b) 40 mb, (c) 50 mb, (d) 60 mb, (e) all others.

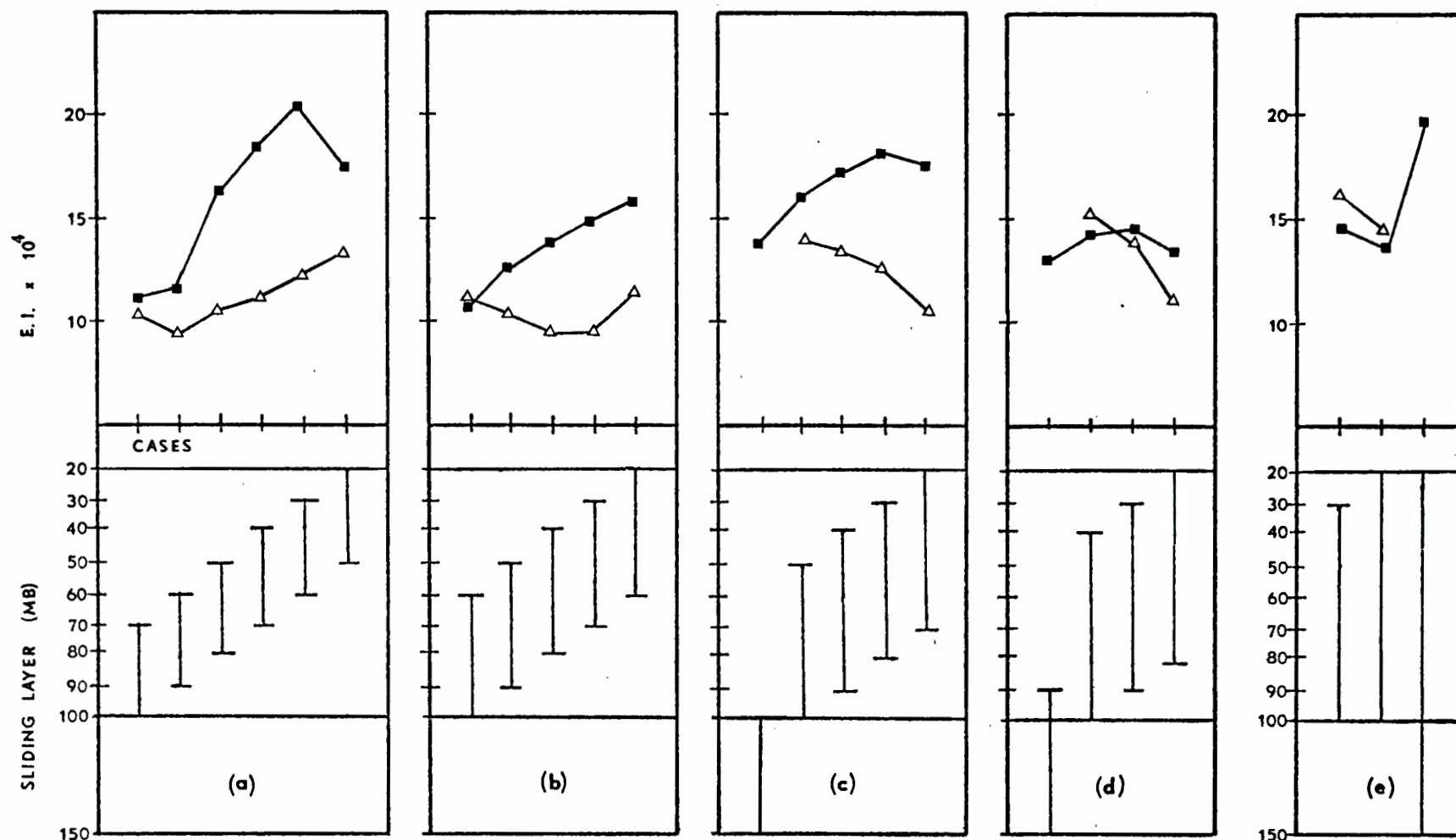


FIG. 16. Cases of stratospheric sub-layer combinations considered and corresponding error index values (35 N to 45 N).

■ E.I. values with tropopause at 150 mb. △ E.I. values with tropopause at 100 mb.
 (a) Sub-layer combinations formed by sliding layer of 30 mb,
 (b) 40 mb, (c) 50 mb, (d) 60 mb, (e) all others.

VII. CONCLUSIONS

This thesis has demonstrated that atmospheric thicknesses can be retrieved from VTPR "clear-column" carbon dioxide radiances by an improved iterative technique for direct solution of the radiative transfer equation, and that systematic errors in the retrieval results can be corrected by selective adjustment of the transmittances. In addition, the retrieved thicknesses of certain standard layers appear to be better specified than others when the "clear column" radiances are used as regression predictors. Furthermore, it has been found in this case that specification of the full troposphere and stratosphere layers can in some instances be improved by decomposition of the layer into sequential pressure intervals.

It should be noted that the study conducted here bears more heavily on the retrieval technique, and utilizes simulated atmospheric-layer thicknesses which have had "clear-column" radiances built into them. In order to make any final inferences as to choice of an optimum layer thickness, the procedure suggested here would have to be conducted over a period of time and retrieved thicknesses verified against thicknesses computed from corresponding radiosonde soundings.

APPENDIX A

CLIMATOLOGICAL TEMPERATURE PROFILES USED TO DERIVE FIRST
GUESS PROFILES FOR VTPR "CLEAR COLUMN" SCAN SPOTS 15N TO 45N

LEVEL	PRESSURE	15N ANN	30N JAN	30N JUL	45N JAN	45N JUL
1	0.010	184.50	191.40	180.30	210.20	174.20
2	0.015	190.90	197.50	187.00	215.30	180.10
3	0.020	196.20	203.10	192.60	219.10	186.00
4	0.025	200.90	206.70	197.10	222.00	191.50
5	0.030	204.80	210.90	201.80	224.50	196.20
6	0.040	210.90	215.70	208.10	228.50	204.10
7	0.050	215.60	220.00	213.00	231.70	210.00
8	0.060	219.60	224.20	217.60	234.30	215.20
9	0.070	223.00	227.10	221.30	236.40	219.10
10	0.085	226.60	231.10	225.50	239.40	224.60
11	0.090	228.90	232.20	227.30	240.20	226.10
12	0.100	232.10	234.40	231.00	242.70	230.60
13	0.150	242.00	243.40	240.50	247.70	243.90
14	0.200	248.90	260.00	248.10	251.80	251.70
15	0.250	254.50	254.40	254.80	255.10	255.90
16	0.300	257.00	257.30	258.40	257.80	259.10
17	0.400	261.30	261.40	262.40	262.40	264.40
18	0.500	264.80	265.00	266.00	265.20	268.80
19	0.600	267.60	267.80	268.90	265.60	272.40
20	0.700	269.80	269.10	271.30	265.60	275.00
21	0.850	270.20	269.20	272.20	265.60	275.70
22	0.900	270.20	269.20	272.20	265.40	275.70
23	1.000	270.20	269.20	272.20	264.50	275.70
24	1.500	265.30	262.20	267.30	254.90	272.60
25	2.000	260.80	258.40	262.50	248.30	267.00
26	2.500	257.00	254.00	259.00	243.40	262.60
27	3.000	254.10	250.30	255.30	239.10	259.60
28	4.000	249.70	245.40	250.40	233.10	253.90
29	5.000	246.00	242.00	246.50	228.50	249.80
30	6.000	243.10	238.50	243.10	224.80	246.40
31	7.000	240.50	236.20	240.70	221.70	243.90
32	8.500	237.90	233.10	238.50	218.70	240.50
33	9.000	237.00	232.20	235.70	218.40	239.20
34	10.000	235.00	230.80	234.10	217.90	237.50
35	15.000	229.00	225.40	229.50	215.90	231.70
36	20.000	224.20	221.40	225.80	215.20	227.50
37	25.000	221.60	218.70	222.40	215.20	225.60
38	30.000	219.20	216.70	220.30	215.20	224.40
39	40.000	214.80	212.80	216.40	215.20	222.10
40	50.000	209.00	209.50	213.90	215.20	220.30
41	60.000	204.30	206.20	211.40	215.20	219.00
42	70.000	200.20	204.30	209.20	215.50	217.80
43	85.000	197.20	203.20	206.40	216.10	216.50
44	90.000	195.50	203.30	205.70	216.30	215.90
45	100.000	196.10	205.50	204.50	216.60	215.70
46	150.000	209.70	211.50	208.20	217.90	215.70
47	200.000	220.40	216.00	221.00	218.80	221.90
48	250.000	230.60	224.80	231.40	219.60	229.30
49	300.000	239.00	233.00	240.40	225.80	238.10
50	400.000	254.90	246.00	255.30	237.60	253.00
51	500.000	264.10	256.80	266.80	247.30	262.40
52	600.000	273.60	266.20	274.70	255.00	272.00
53	700.000	282.70	274.30	282.20	261.90	278.80
54	850.000	290.50	282.60	290.30	267.10	287.30
55	900.000	293.40	284.00	293.30	268.70	289.50
56	1000.000	299.10	286.30	300.60	271.60	293.80

The following procedure was used to expand standard 56 level climatological temperature profiles to 100 level profiles on the J scale:

1. Where pressures of J-levels were equal to pressures of standard levels, the temperature at the J-level was set equal to the temperature at the standard level.

2. Where pressures of J-levels were not equal to pressures of standard levels, temperatures at the J-levels were computed by interpolation as follows:

$$T(J) = T_{STD}(M-1) + \left[\frac{T_{STD}(M) - T_{STD}(M-1)}{P_{STD}(M) - P_{STD}(M-1)} \right] [P(J) - P_{STD}(M-1)]$$

where

$T(J)$ = desired temperature at the J-level

$P(J)$ = pressure at the J-level

$T_{STD}(M-1)$ = known temperature at nearest standard pressure level above the J-level

$T_{STD}(M)$ = known temperature at nearest standard pressure level below the J-level

$P_{STD}(M-1)$
 $P_{STD}(M)$ = pressures at nearest standard levels above and below the J-level.

UNTUNED TRANSMITTANCES AND CORRESPONDING STANDARD TEMPERATURES
AND J-SCALE PRESSURES FOR THE SIX VTPR "CLEAR COLUMN"
CARBON DIOXIDE CHANNELS

LEVEL	PRESSURE	TEMP	CHAN 1	CHAN 2	CHAN 3	CHAN 4	CHAN 5	CHAN 6
1	0.010	180.65	.992320	.998510	.999322	.999939	.999942	.999995
2	0.023	196.37	.990063	.998136	.999042	.999843	.999853	.999987
3	0.043	212.09	.987048	.997523	.998636	.999654	.999678	.999967
4	0.076	227.73	.982813	.996643	.998205	.999280	.999339	.999914
5	0.122	242.46	.977742	.995518	.997612	.998774	.998878	.999817
6	0.186	254.87	.972025	.994192	.996870	.998207	.998359	.999678
7	0.270	261.55	.965256	.992722	.995555	.997634	.997834	.999490
8	0.379	264.27	.956992	.991074	.994957	.997080	.997328	.999254
9	0.517	267.16	.946836	.988987	.993811	.996472	.996788	.998989
10	0.687	270.40	.934678	.986343	.992427	.995782	.996190	.998715
11	0.893	271.18	.920520	.983262	.990890	.995053	.995556	.998449
12	1.140	269.21	.904340	.979704	.989170	.994279	.994869	.998193
13	1.432	265.12	.886238	.975581	.987225	.993450	.994108	.997944
14	1.775	260.39	.866456	.970848	.985053	.992574	.993273	.997699
15	2.172	256.16	.845325	.965418	.982617	.991627	.992343	.997449
16	2.629	252.17	.823277	.959213	.979884	.990585	.991301	.997186
17	3.151	248.46	.800772	.952150	.976822	.989444	.990136	.996906
18	3.743	244.98	.778183	.944153	.973356	.988177	.988835	.996602
19	4.410	241.70	.755801	.935145	.969585	.986783	.987397	.996272
20	5.158	238.63	.733744	.925057	.965366	.985259	.985822	.995913
21	5.993	235.74	.711956	.913824	.960714	.983596	.984104	.995524
22	6.921	232.88	.690273	.901381	.955618	.981798	.982251	.995104
23	7.946	230.32	.668459	.887672	.950058	.979860	.980262	.994652
24	9.076	228.58	.646231	.872649	.943590	.977762	.978126	.994162
25	10.316	227.46	.623379	.856268	.937365	.975478	.975827	.993627
26	11.672	226.63	.599778	.838491	.930133	.972983	.973353	.993039
27	13.152	225.89	.575426	.819289	.922269	.970268	.970705	.992396
28	14.760	225.13	.550353	.798645	.913751	.967323	.967886	.991696
29	16.505	224.38	.524640	.776552	.904559	.964141	.964900	.990937
30	18.392	223.67	.498389	.753023	.894676	.960711	.961752	.990118
31	20.428	222.99	.471718	.728088	.884083	.957026	.958449	.989236
32	22.621	222.33	.444755	.701800	.872768	.953079	.955002	.988291
33	24.976	221.69	.417640	.674230	.860716	.948862	.951417	.987281
34	27.502	221.06	.390520	.645477	.847517	.944367	.947705	.986205
35	30.206	220.46	.363544	.615663	.834356	.939583	.943869	.985061
36	33.094	219.88	.336861	.584931	.820022	.934497	.939912	.983847
37	36.174	219.31	.310613	.553440	.804913	.929103	.935839	.982560
38	39.453	218.74	.284939	.521367	.789038	.923396	.931655	.981202
39	42.939	218.16	.259576	.488918	.772406	.917373	.927361	.979771
40	46.641	217.62	.235839	.456293	.755021	.911020	.922953	.978265
41	50.564	217.18	.212633	.423695	.736878	.904317	.918421	.976677

APPENDIX B

42	54.718	216.89	.190454	.391333	.717976	.897241	.913750	.975002
43	59.110	216.73	.169373	.359398	.698326	.889775	.908934	.973234
44	63.749	216.66	.149458	.328072	.677542	.881901	.903961	.971368
45	68.641	216.64	.130774	.297525	.656844	.873596	.898819	.969398
46	73.796	216.64	.113373	.267922	.635063	.864847	.893498	.967317
47	79.223	216.65	.097297	.239406	.612644	.855642	.887989	.965123
48	84.928	216.66	.082586	.212100	.589641	.845970	.882283	.962811
49	90.920	216.66	.069261	.186148	.566115	.835825	.876373	.960378
50	97.209	216.65	.057334	.161684	.542141	.825204	.870253	.957822
51	103.803	216.64	.046815	.138812	.517803	.814104	.863915	.955141
52	110.710	216.64	.037667	.117645	.493188	.802525	.857351	.952331
53	117.939	216.63	.029814	.098305	.468379	.790462	.850556	.949390
54	125.499	216.64	.023179	.080879	.443469	.777912	.843521	.946314
55	133.399	216.66	.017684	.065410	.418559	.764876	.836237	.943099
56	141.648	216.69	.013230	.051908	.393752	.751357	.828699	.939743
57	150.255	216.70	.009681	.040357	.369151	.737366	.820906	.936245
58	159.230	216.65	.006926	.030679	.344865	.722919	.812856	.932605
59	168.581	216.55	.004821	.022736	.321001	.708031	.804551	.928824
60	178.317	216.46	.003262	.016410	.297644	.692692	.795978	.924892
61	188.449	216.45	.002145	.011541	.274865	.676882	.787121	.920794
62	198.986	216.63	.001367	.007894	.252726	.660573	.777961	.916516
63	209.937	217.06	.000832	.005180	.231282	.643730	.768472	.912035
64	221.312	217.78	.000482	.003250	.210592	.626298	.758619	.907319
65	233.120	218.82	.000270	.001982	.190706	.608208	.748360	.902328
66	245.372	220.20	.000152	.001207	.171666	.589376	.737642	.897012
67	258.076	221.94	.000084	.000718	.153495	.569706	.726407	.891317
68	271.244	223.98	.000042	.000358	.136245	.549161	.714616	.885199
69	284.885	226.18	.000020	.000209	.119990	.527753	.702244	.878625
70	299.010	228.42	.000009	.000107	.104796	.505506	.689270	.871561
71	313.627	230.61	.000002	.000044	.090718	.482456	.675672	.863973
72	328.747	232.73	.0	.000003	.077797	.458673	.661443	.855839
73	344.382	234.79	.0	.0	.066057	.434249	.646583	.847146
74	360.540	236.81	.0	.0	.055507	.409258	.631098	.837882
75	377.232	238.82	.0	.0	.046132	.383959	.614996	.828038
76	394.470	240.81	.0	.0	.037895	.358397	.598293	.817607
77	412.263	242.81	.0	.0	.030737	.332801	.581011	.806588
78	430.622	244.83	.0	.0	.024604	.307336	.563170	.794979
79	449.557	246.84	.0	.0	.019439	.282149	.544794	.782780
80	469.080	248.86	.0	.0	.015161	.257409	.525913	.769995
81	489.201	250.87	.0	.0	.011659	.233306	.506564	.756632
82	509.931	252.87	.0	.0	.008792	.210047	.486790	.742707
83	531.283	254.85	.0	.0	.006460	.187796	.466639	.728228
84	553.263	256.83	.0	.0	.004627	.166645	.446155	.713196
85	575.887	258.79	.0	.0	.003245	.146685	.425392	.697618
86	599.164	260.75	.0	.0	.002252	.128006	.404411	.681500
87	623.105	262.69	.0	.0	.001571	.110692	.383281	.664854
88	647.721	264.63	.0	.0	.001108	.094828	.362083	.647696
89	673.025	266.57	.0	.0	.000761	.080482	.340904	.630047

90	699.028	268.50	.0	.0	.000500	.067656	.319817	.611931
91	725.737	270.42	.0	.0	.000313	.056310	.298899	.593374
92	753.171	272.33	.0	.0	.000188	.046382	.278231	.574411
93	781.335	274.24	.0	.0	.000111	.037785	.257905	.555083
94	810.246	276.15	.0	.0	.000062	.030400	.238018	.535436
95	839.911	278.04	.0	.0	.000030	.024124	.218666	.515515
96	870.346	279.94	.0	.0	.000009	.018896	.199926	.495360
97	901.559	281.82	.0	.0	.0	.014638	.181881	.475013
98	933.565	283.70	.0	.0	.0	.011253	.164618	.454524
99	966.374	285.57	.0	.0	.0	.008618	.148227	.433947
100	999.997	287.42	.0	.0	.0	.006586	.132805	.413343

ITERATIVE TECHNIQUE FOR RETRIEVAL OF
LAYER MEAN TEMPERATURES FROM NOAA-II
VTPR "CLEAR COLUMN" RADIANCE DATA.

LT DOUGLAS R. MGRAN
NAVAL POSTGRADUATE SCHOOL
NOVEMBER 1973

DIMENSION ARRAYS

DIMENSION PSTD(56),TSTD(56),P(103),T(106),TAU(6,106),C
1 HAN(6),B(6,106),AVCHAN(103),BMEAN(6,106),RDIFF(6),RDIF
2 FA(6),TGUESS(103),RADCBS(7),RADCCM(6),DT(6,106),RADATM
3 (6),RADSF(6),TREF(5,106),TDIFF(103)

DEFINE FCN STATEMENTS FOR BAILEY ITERATIVE SOLN OF
PLANCK FCN FOR REF WAVE NOS

F(X)=C1*X**3-BREF*EXP(C2*X/TEMP)+BREF
DF(X)=3.0*C1*X**2-BREF*(C2/TEMP)*EXP(C2*X/TEMP)
DDF(X)=6.0*C1*X-BREF*(C2/TEMP)*(C2/TEMP)*EXP(C2*X/TEMP
1)

SET DATA AND ZERO OUT ARRAYS

DATA PI/3.1415927/,C1/0.000037403/,C2/1.43868/,F1/0.16
166667/,F2/0.6666667/,EPSREF/0.05/,EPSRAD/0.0001/,TW05/
22.5/,NTEN/10/,LAT25/25/,LAT35/35/,LAT45/45/,T/106*C./,
3 TAU/636*0./,B/636*0./,BMEAN/636*0./
C1=C1/PI

READ SIX CG2 CHANNEL WAVE NOS, 56 LEVEL PRESS AND TEMP
FOR 15, 30, 45 N LAT STD PROFILES, TRANSMITTANCE VALUE
FOR 100 LEVELS

READ (5,36) (CHAN(N),N=1,6)
READ (5,38) (PSTD(J),J=1,56)
DO 1 N=1,5
READ (5,39) (TREF(N,J),J=1,56)
1 CONTINUE
DO 2 N=1,6
READ (5,37) (TAU(N,I),I=1,100)
2 CONTINUE

INTERPOLATE FOR "APRIL" STD TEMP PROFILES AT 30 AND 45
N LAT FROM JAN AND JUL STD PROFILES

DO 3 J=1,56
TREF(2,J)=(TREF(2,J)+TREF(4,J))*0.5
TREF(3,J)=(TREF(3,J)+TREF(5,J))*0.5
3 CONTINUE

COMPUTE PRESS FOR 100 LEVELS AND TUNE TRANSMITTANCES

DO 4 I=1,100
P(I)=0.01*(1.0+(I-1)*0.26087836)**3.5
TAU(5,I)=0.95*TAU(5,I)
TAU(6,I)=0.90*TAU(6,I)
4 CONTINUE

COMPUTE LAYER TRANSMITTANCES

DO 6 N=1,6
DO 5 I=7,103,6
DT(N,I)=TAU(N,I-3)-TAU(N,I+3)
IF (I.EQ.103) DT(N,I)=TAU(N,I)-TAU(N,4)
5 CONTINUE
6 CONTINUE


```

C      WRITE (6,56)
C      WRITE (6,55) (DT(N,103),N=1,6),((DT(N,I),N=1,6),I=7,97
1,6)
C      READ LAT, LONG, RADIANCES, SEA SFC TEMP FOR SCAN SPOT
C      7 READ (5,40,END=35) ALAT,ALONG,(RADCBS(N),N=1,6),TSFC
C      CONVERT LAT, LONG, RADIANCES TO CORRECT DIMENSIONS
C      LATREF=30
C      ALAT=ALAT*0.1-90.0
C      ALONG=ALONG*0.1
C      DO 8 N=1,6
C      RADOBS(N)=RADCBS(N)*0.05
8 CONTINUE
C      INTERPOLATE FOR 56 LEVEL PROFILE AT LAT OF SCAN SPOT
C      FROM "APRIL" STD PROFILES N AND S OF SCAN SPOT
C      IF (ALAT.LT.LATREF) LATREF=15
C      FACLAT=(ALAT-LATREF)/15.0
C      LAT=LATREF/15
C      LATP1=LAT+1
C      DO 9 J=1,56
C      TSTD(J)=FACLAT*(TREF(LATP1,J)-TREF(LAT,J))+TREF(LAT,J)
C      IF (ALAT.EQ.LATREF) TSTD(J)=TREF(LAT,J)
9 CONTINUE
C      SET 1000MB TEMP EQ TO OBSERVED SEA SFC TEMP
C      TSTD(56)=TSFC*0.2+269.9
C      EXPAND 56 LEVEL PROFILE FOR SCAN SPOT TO 100 LEVELS
C      DO 12 I=1,100
C      STEP DOWN THRU 56 LEVEL PROFILE UNTIL PRESS EQ OR GT
C      CURRENT 100 LEVEL PRESS
C      DO 10 J=1,56
C      IF PRESS EQ SET TEMPS EQ, IF PRESS GT INTERPOLATE FOR
C      TEMP
C      IF (PSTD(J).EQ.P(I)) T(I)=TSTD(J)
C      IF (PSTD(J).GT.P(I)) GO TO 11
10 CONTINUE
C      BEGIN INTERPOLATION ROUTINE
11 K=J-1
C      RATIO=(TSTD(J)-TSTD(K))/(PSTD(J)-PSTD(K))
C      PDIFF=P(I)-PSTD(K)
C      T(I)=TSTD(K)+(RATIO*PDIFF)
C      END INTERPOLATION ROUTINE
12 CONTINUE
C      WRITE (6,50) ALAT,ALONG
C      WRITE (6,51)
C      COMPUTE PRESS AND TEMP OF J=2.5 LEVEL TO COMPLETE
C      FIRST GUESS PROFILE FOR SCAN SPOT
C      P(103)=0.01*(1.0+(1.5)*0.26087836)**3.5
C      T(103)=T(2)+((T(3)-T(2))/(P(3)-P(2)))*(P(103)-P(2))
C      DO 13 J=1,25
C      J25=J+25
C      J50=J+50
C      J75=J+75
C      WRITE (6,49) (J,P(J),T(J),J25,P(J25),T(J25),J50,P(J50)
1,T(J50),J75,P(J75),T(J75))
13 CONTINUE

```

```

C      COMPUTE PLANCK VALUES FOR ALL CHANNELS AND REQUIRED
C      PRESS LEVELS USING FIRST GUESS PROFILE
C
DO 15 N=1,6
DO 14 I=1,103,3
B(N,I)=(C1*CHAN(N)**3)/(EXP(C2*CHAN(N)/T(I))-1)
TGUESS(I)=T(I)
14 CONTINUE
15 CCNTINUE

C      COMPUTE LAYER MEAN PLANCK VALUES
C
DO 17 I=7,103,6
DO 16 N=1,6
BMEAN(N,I)=F1*B(N,I-3)+F2*B(N,I)+F1*B(N,I+3)
IF (I.EQ.103) BMEAN(N,I)=F1*B(N,1)+F2*B(N,103)+F1*B(N,
14)
16 CCNTINUE
17 CONTINUE

C      CALCULATE RADIANCES FOR FIRST GUESS PROFILE
C
DC 19 N=1,6
RADSFC(N)=8(N,100)*TAU(N,100)
RADATM(N)=0.0
DC 18 I=7,103,6
RAD=BMEAN(N,I)*DT(N,I)
RADATM(N)=RADATM(N)+RAD
18 CONTINUE
RADCOM(N)=RADATM(N)+RADSFC(N)
RCIFF(N)=RADOBS(N)-RADCOM(N)
RDIFFA(N)=ABS(RADOBS(N)-RADCOM(N))/RADOBS(N)
19 CONTINUE

C      COMPUTE REF WAVE NO FOR EACH LAYER USING WEIGHTED
C      LAYER MEAN PLANCK VALUES AND BAILEY ITERATION METHOD
C
DC 22 I=7,103,6
KCUNT=0
SUMBDT=0.0
SUMDT=0.0
DC 20 N=1,6
BDT=BMEAN(N,I)*DT(N,I)
SUMBDT=SUMBDT+BDT
SUMDT=SUMDT+DT(N,I)
20 CCNTINUE
BREF=SUMBDT/SUMDT

C      BEGIN BAILEY ITERATIVE TECHNIQUE
C
X1=665.0+I
IF (I.EQ.103) X1=670.0
TEMP=F1*T(I-3)+F2*T(I)+F1*T(I+3)
IF (I.EQ.103) TEMP=F1*T(1)+F2*T(103)+F1*T(4)
21 X2=X1-(F(X1)/(DF(X1)-(F(X1)*DDF(X1)/(2.*DF(X1)))))
DIFF=ABS(X2-X1)
X1=X2
KCUNT=KCUNT+1
IF (DIFF.GT.EPSREF) GO TO 21
AVCHAN(I)=X2
END BAILEY ITERATIVE TECHNIQUE

C      22 CCNTINUE
C
WRITE (6,53) TWO5,(I,I=7,97,6)
WRITE (6,54) AVCHAN(103),(AVCHAN(I),I=7,97,6)
WRITE (6,47) ALAT,ALONG
WRITE (6,46) (RADOBS(N),N=1,6)
WRITE (6,43)
WRITE (6,46) (RADCOM(N),N=1,6)

C      COMPARE OBSERVED AND CALCULATED RADIANCES AND ADJUST
C      LAYER MEAN PLANCK VALUES

```

```

C
23 KCUNT=0
   KCUNT=KCUNT+1
   DO 25 N=1,6
     RDIFF(N)=RADOBS(N)-RADCOM(N)
     RDIFFA(N)=ABS(RDIFF(N)/RADOBS(N))
     DO 24 I=7,103,6
       BMEAN(N,I)=BMEAN(N,I)+RDIFF(N)
24  CONTINUE
25  CONTINUE

C
C   CALCULATE RADIANCES USING ADJUSTED LAYER MEAN PLANCKS
C
   DO 27 N=1,6
     RADATM(N)=0.0
     DO 26 I=7,103,6
       RAD=BMEAN(N,I)*DT(N,I)
       RADATM(N)=RADATM(N)+RAD
26  CONTINUE
     RADCOM(N)=RADATM(N)+RADSF(N)
27  CONTINUE

C
   WRITE (6,44)
   WRITE (6,46) (RDIFF(N),N=1,6)
   WRITE (6,46) (RDIFFA(N),N=1,6)
   WRITE (6,45) KCUNT
   WRITE (6,46) (RADCOM(N),N=1,6)

C
C   COMPARE DIFFERENCE BETWEEN OBSERVED AND CALCULATED
C   RADIANCES AGAINST CONVERGENCE CRITERION
C
   DO 28 N=1,6
     RDIFF(N)=RADOBS(N)-RADCOM(N)
     RDIFFA(N)=ABS(RADOBS(N)-RADCOM(N))/RADOBS(N)
     IF (KCUNT.EQ.NTEN) GO TO 29
     IF (RDIFFA(N).GT.EPSRAD) GO TO 23
28  CONTINUE

C
   GO TO 30
29  WRITE (6,52)

C
30  WRITE (6,44)
   WRITE (6,46) (RDIFF(N),N=1,6)
   WRITE (6,46) (RDIFFA(N),N=1,6)

C
C   COMPUTE LAYER MEAN TEMPS FROM FINAL LAYER MEAN PLANCKS
C
   DO 32 I=7,103,6
     SUMDT=0.0
     SUMBDT=0.0
     DO 31 N=1,6
       BDT=BMEAN(N,I)*DT(N,I)
       SUMBDT=SUMBDT+BDT
       SUMDT=SUMDT+DT(N,I)
31  CONTINUE
     BREF=SUMBDT/SUMDT
     T(I)=(C2*AVCHAN(I))/ALOG((C1*AVCHAN(I)**3+BREF)/BREF)
32  CONTINUE

C
C   INTERPOLATE FOR TEMPS AT INTERMEDIATE LEVELS
C
   DO 33 I=10,94,6
     T(I)=(T(I-3)+T(I+3))*0.5
33  CONTINUE
     T(4)=(T(103)+T(7))*0.5
     T(1)=T(103)-(T(4)-T(103))

C
C   COMPUTE DIFFERENCE BETWEEN FIRST GUESS AND RETRIEVED
C   TEMP PROFILES
C
   DO 34 I=1,100,3
     TDIFF(I)=T(I)-TGUESS(I)

```

```

C 34 CONTINUE
C   WRITE (6,48) ALAT,ALONG,KOUNT
C   WRITE (6,42)
C   WRITE (6,41) (I,P(I),T(I),TDIFF(I),I=1,100,3)
C
C   COMPUTE RADIANCE FOR WINDOW CHANNEL FROM SEA SFC TEMP
C   RADOBS(7)=(C1*835.**3)/(EXP(C2*835./TSTD(56))-1)
C
C   LBAND=1
C   IF ((ALAT.GE.LAT25).AND.(ALAT.LT.LAT35)) LBAND=2
C   IF ((ALAT.GE.LAT35).AND.(ALAT.LT.LAT45)) LBAND=3
C
C   PUNCH CARDS FOR THICKNESS PROGRAMS
C   WRITE (7,57) LBAND,ALAT,ALONG,T(1),T(103),(T(I),I=7,97
C   1,6),T(100),(RADOBS(N),N=1,7)
C
C   GC TO 7
C
C 35 STOP
C
C 36 FORMAT (6F6.1)
C 37 FORMAT (8F10.8)
C 38 FORMAT (8F10.4)
C 39 FORMAT (10F8.3)
C 40 FORMAT (9F7.1)
C 41 FORMAT (' ',T24,I3,T53,F10.4,T84,F8.3,T114,F8.3)
C 42 FORMAT (' ',T24,'LEVEL',T57,'PRESS',T85,'TEMP',T109,'R
C 1INITIAL',/)
C 43 FORMAT ('0',/,T10,'COMPUTED RADIANCES FROM FIRST GUESS
C 44 FORMAT (' ',T10,'RADIANCE RESIDUALS')
C 45 FORMAT ('0',T10,'COMPUTED RADIANCES AT ITERATION NO.',
C 46 FORMAT (' ',T10,6F12.6)
C 47 FORMAT ('0',T10,'OBSERVED RADIANCES',5X,'N. LAT',F7.1,
C 1,F7.1)
C 48 FORMAT ('0',///,T10,'RETRIEVED TEMP PROFILE',5X,'N. LA
C 1W. LONG',F7.1,T80,'NO OF ITERATIONS NEEDED',I7,/)
C 49 FORMAT (' ',4(8X,I3,4X,F7.3,4X,F7.3))
C 50 FORMAT ('0',/,T10,'STD TEMP PROFILE',5X,'N. LAT',F7.1,
C 1,F7.1)
C 51 FORMAT ('0',4(8X,'LEVEL',4X,'PRESS',4X,'TEMP',3X))
C 52 FORMAT ('0',/,T10,'ITERATIONS TERMINATED AT 10, FRACTI
C 1E, CBSERVED - COMPUTED RADIANCES, FOLLOWS')
C 53 FORMAT ('0',/,T10,'LEVEL NO',T25,F6.1,16I6)
C 54 FORMAT (' ',T10,'REF WAVE NO',T25,17F6.1)
C 55 FORMAT (' ',T10,6F12.5)
C 56 FORMAT ('0',///,T10,'LAYER TRANSMITTANCES',/)
C 57 FORMAT (I1,9X,10F7.2/(3X,11F7.2)/(7F9.2))
C
C   END

```

STD TEMP PROFILE N. LAT 19.2 W. LONG 63.0

LEVEL	PRESS	TEMP	LEVEL	PRESS	TEMP	LEVEL	PRESS	TEMP	LEVEL	PRESS	TEMP
1	0.010	184.878	26	11.672	232.373	51	103.803	199.440	76	394.470	252.861
2	0.023	158.929	27	13.152	230.680	52	110.710	200.980	77	412.263	254.905
3	0.043	212.802	28	14.760	228.840	53	117.939	202.592	78	430.622	256.694
4	0.076	224.741	29	16.505	227.201	54	125.459	204.278	79	449.557	258.540
5	0.122	236.542	30	18.392	225.490	55	133.399	206.040	80	469.080	260.442
6	0.186	247.962	31	20.428	223.798	56	141.648	207.880	81	489.201	262.403
7	0.270	255.632	32	22.621	222.603	57	150.255	209.794	82	509.931	264.375
8	0.379	260.599	33	24.976	221.319	58	159.230	211.611	83	531.283	266.353
9	0.517	265.471	34	27.502	220.154	59	168.581	213.505	84	553.263	268.389
10	0.687	269.630	35	30.206	218.916	60	178.317	215.477	85	575.887	270.484
11	0.893	270.340	36	33.094	217.686	61	188.449	217.529	86	599.164	272.640
12	1.140	266.887	37	36.174	216.374	62	198.566	219.663	87	623.105	274.736
13	1.432	265.849	38	39.453	214.977	63	209.937	221.862	88	647.721	276.887
14	1.775	262.704	39	42.939	213.278	64	221.312	224.144	89	673.025	279.097
15	2.172	259.381	40	46.641	211.432	65	233.120	226.513	90	699.028	281.369
16	2.629	256.055	41	50.564	209.515	66	245.372	228.971	91	725.737	283.811
17	3.151	253.052	42	54.718	207.776	67	258.076	231.266	92	753.171	286.258
18	3.743	250.364	43	59.110	205.933	68	271.244	233.493	93	781.335	288.744
19	4.410	247.685	44	63.749	204.238	69	284.885	235.800	94	810.246	291.269
20	5.158	245.026	45	68.641	202.513	70	299.010	238.188	95	839.911	293.833
21	5.993	242.476	46	73.796	201.345	71	313.627	240.448	96	870.346	296.466
22	6.921	240.127	47	79.223	200.370	72	328.747	242.770	97	901.559	299.192
23	7.946	238.277	48	84.928	199.341	73	344.382	245.170	98	933.565	302.008
24	9.076	236.005	49	90.920	198.073	74	360.540	247.651	99	966.374	304.927
25	10.316	233.925	50	97.209	196.432	75	377.222	250.214	100	999.997	307.999

LEVEL NO 2.5 7 13 19 25 31 37 43 49 55 61 67 73 79 85 91 97
 REF WAVE NO 668.4 609.2 675.1 676.8 679.4 681.0 682.7 685.3 690.1 696.4 704.0 709.9 714.5 719.3 723.8 728.9 733.4

OBSERVED RADIANCES N. LAT 19.2 W. LONG 63.0
 54.449982 44.349991 41.949997 59.399994 80.149554 98.059991

COMPUTED RADIANCES FROM FIRST GUESS PROFILE
 55.406097 43.703049 43.967941 65.803513 82.943344 99.306531
 RADIANCE RESIDUALS
 -0.956116 0.646942 -2.017944 -6.403519 -2.793350 -1.206940
 0.017560 0.014587 0.048104 0.107803 0.034852 0.012303

COMPUTED RADIANCES AT ITERATION NO. 1
 54.457306 44.245045 41.951385 59.442535 80.642242 98.666693
 RADIANCE RESIDUALS
 -0.007324 0.000946 -0.001389 -0.042542 -0.492249 -0.565702
 0.000135 0.000021 0.000033 0.000716 0.006142 0.005607

COMPUTED RADIANCES AT ITERATION NO. 2
 54.450073 44.249991 41.949997 59.400269 80.236755 98.368896
 RADIANCE RESIDUALS
 -0.000092 0.0 0.0 -0.000275 -0.086761 -0.268906
 0.000002 0.0 0.0 0.000005 0.001062 0.002741

COMPUTED RADIANCES AT ITERATION NO. 3
 54.449566 44.249991 41.949997 59.399994 80.165268 98.226898
 RADIANCE RESIDUALS
 0.000015 0.0 0.0 0.0 -0.015274 -0.126507
 0.000000 0.0 0.0 0.0 0.000191 0.001294

COMPUTED RADIANCES AT ITERATION NO. 4
 54.449982 44.249991 41.949997 59.399994 80.152695 98.159912
 RADIANCE RESIDUALS
 0.0 0.0 0.0 0.0 -0.002701 -0.055521
 0.0 0.0 0.0 0.0 0.000034 0.000611

COMPUTED RADIANCES AT ITERATION NO.			5		
54.449982	44.349991	41.949997	59.399994	80.150482	98.128250
RADIANCE RESIDUALS					
0.0	0.0	0.0	0.0	-0.000488	-0.028259
0.0	0.0	0.0	0.0	0.000006	0.000288

COMPUTED RADIANCES AT ITERATION NO.			6		
54.449982	44.349991	41.949997	59.399994	80.150085	98.113342
RADIANCE RESIDUALS					
0.0	0.0	0.0	0.0	-0.000052	-0.013351
0.0	0.0	0.0	0.0	0.000001	0.000136

COMPUTED RADIANCES AT ITERATION NO.			7		
54.449982	44.349991	41.949997	59.399994	80.149979	98.106293
RADIANCE RESIDUALS					
0.0	0.0	0.0	0.0	0.000015	-0.006302
0.0	0.0	0.0	0.0	0.000000	0.000064

RETRIEVED TEMP PROFILE	N. LAT	19.2	W. LONG	63.0	NO OF ITERATIONS NEEDED	7
LEVEL			PRESS		TEMP	RETRIEVED - INITIAL
1			0.0100		179.144	-5.724
4			0.0756		227.612	-2.871
7			0.2704		251.847	-3.786
10			0.6866		257.968	-11.662
13			1.4323		264.085	-1.760
16			2.6289		255.544	-0.511
19			4.4101		246.998	-0.686
22			6.5206		240.104	-0.023
25			10.3158		233.205	-0.716
28			14.7604		228.108	-0.732
31			20.4283		223.007	-0.792
34			27.5024		218.983	-1.171
37			36.1735		214.959	-1.415
40			46.6406		205.674	-1.758
43			59.1102		204.388	-1.545
46			73.7565		200.471	-0.878
49			90.9201		196.553	-1.520
52			110.7097		159.698	-1.282
55			133.3590		202.844	-3.196
58			159.2296		208.301	-3.310
61			188.4454		213.758	-3.771
64			221.3121		220.504	-3.640
67			258.0764		227.249	-4.017
70			299.0095		234.356	-3.792
73			344.3816		241.544	-3.627
76			394.4705		248.356	-4.505
79			449.5566		255.169	-3.371
82			509.9314		261.384	-2.991
85			575.8867		267.600	-2.885
88			647.7214		273.890	-2.996
91			725.7373		280.181	-2.630
94			810.2458		285.457	-1.812
97			901.5591		290.732	-1.459
100			999.9971		295.899	0.0

CONVERSION OF RETRIEVED LAYER MEAN
TEMPERATURES TO ATMOSPHERIC THICKNESSES
FOR "STANDARD" TROPOSPHERIC LAYERS.

LT DOUGLAS R. MORAN
NAVAL POSTGRADUATE SCHOOL
DECEMBER 1973

DIMENSION ARRAYS

DIMENSION PSTD(60), TSTD(60), P(19), T(19), DZ(59), Y1
1(8), Y2(8), RADOBS(7)

SET DATA

DATA R/28700./,G/980./,LBAND1/0/,LBAND2/0/,LBAND3/0/,N
1ONE/1/,NTWC/2/,NTHREE/3/
RG=R/G

READ IN MEAN PRESS LEVELS FROM 100 LEVEL PROFILE AND
STD LEVELS FOR 56 LEVEL PROFILE AND ADDITIONAL LEVELS
80, 450, 550, 650, TO COMPLETE "STANDARD" LEVELS

READ (5,11) (PSTD(J),J=1,60)
READ (5,12) (P(I),I=1,19)

READ IN LAT BAND, LAT, LONG, AND TEMPS FOR TOP LAYER
MEANS, SFC, FROM TEMP RETRIEVAL PROGRAM

1 READ (5,13,END=10) LBAND,ALAT,ALONG,(T(I),I=1,19),(RAD
1OBS(N),N=1,7)

EXPAND 19 LEVEL RETRIEVED PROFILE TO 60 LEVELS

DO 4 J=1,60
DO 2 I=1,19
IF (P(I).EQ.PSTD(J)) TSTD(J)=T(I)
IF (P(I).GT.PSTD(J)) GO TO 3

2 CONTINUE

BEGIN INTERPOLATION ROUTINE

3 K=I-1
RATIO=(T(I)-T(K))/(P(I)-P(K))
PDIFF=PSTD(J)-P(K)
TSTD(J)=T(K)+(RATIO*PDIFF)
END INTERPOLATION ROUTINE

4 CONTINUE

IF (LBAND.EQ.NONE) WRITE (6,14) ALAT,ALONG
IF (LBAND.EQ.NONE) WRITE (6,15)

DO 5 J=1,15
J15=J+15
J30=J+30
J45=J+45
IF (LBAND.EQ.NONE) WRITE (6,16) (J,PSTD(J),TSTD(J),J15
1,PSTD(J15),TSTD(J15),J30,PSTD(J30),TSTD(J30),J45,PSTD
2(J45),TSTD(J45))

5 CONTINUE

COMPUTE LAYER THICKNESSES

DO 6 I=1,59
DZ(I)=RG*((TSTD(I+1)+TSTD(I))*0.5)*(ALOG(PSTD(I+1)/PST
1D(I)))
6 CONTINUE


```

C      COMPUTE THICKNESSES ABOVE AND BELOW KEY LEVELS
C      DC 9 M=46,56
C      K=M-45
C      Y2(K)=0.0
C      DO 7 N=46,M
C      Y2(K)=Y2(K)+DZ(N)
7      CONTINUE
C      M1=M+1
C      Y1(K)=0.0
C      DO 8 NN=M1,59
C      Y1(K)=Y1(K)+DZ(NN)
8      CONTINUE
C      PRESS=PSTD(M1)
C      IF (LBAND.EQ.NONE) WRITE (6,17) PRESS,Y2(K)
C      IF (LBAND.EQ.NONE) WRITE (6,18) PRESS,Y1(K)
C      9 CONTINUE
C      IF (LBAND.EQ.NONE) LBAND1=LBAND1+1
C      IF (LBAND.EQ.NTWO) LBAND2=LBAND2+1
C      IF (LBAND.EQ.NTHREE) LBAND3=LBAND3+1
C      PUNCH THICKNESS DATA CARDS FOR LATITUDE BAND ONE FOR
C      ANALYSIS BY BIMED 02R
C      IF (LBAND.EQ.NONE) WRITE (7,20) ALAT,ALONG,(RADOBS(K),
C      1K=1,7)
C      IF (LBAND.EQ.NONE) WRITE (7,21) ALAT,ALONG,(Y2(K),K=1,
C      18)
C      IF (LBAND.EQ.NONE) WRITE (7,21) ALAT,ALONG,(Y1(K),K=1,
C      18)
C      GO TO 1
C      10 WRITE (6,19) LBAND1,LBAND2,LBAND3
C      STCP
C      11 FORMAT (6F10.3)
C      12 FORMAT (10F8.3)
C      13 FORMAT (11,9X,10F7.2/(3X,11F7.2)/(7F9.2))
C      14 FORMAT ('0',/,T10,'60 LEVEL PROFILE',5X,'N. LAT',F7.1,
C      1,F7.1)
C      15 FORMAT ('0',4(8X,'LEVEL',4X,'PRESS',4X,'TEMP',3X))
C      16 FORMAT (' ',4(8X,I3,3X,F8.3,3X,F8.3))
C      17 FORMAT ('0',T10,'THICKNESS',F9.2,' MB TO 100.00 MB =
C      1TERS')
C      18 FORMAT (' ',T10,'THICKNESS 1000.00 MB TO',F8.2,' MB =
C      1ETERS')
C      19 FORMAT ('0',//,T10,'NUMBER OF CASES 15N TO 25N',I5,8X,
C      1ASES 25N TO 35N',I5,8X,'NUMBER OF CASES 35N TO 45N',I5
C      20 FORMAT (2F6.1,7F9.2)
C      21 FORMAT (2F6.1,8F8.1)
C      END

```


60 LEVEL PROFILE N. LAT 19.2 W. LONG 63.0

LEVEL	PRESS	TEMP	LEVEL	PRESS	TEMP
1	C.010	179.140	16	0.300	252.166
2	0.015	184.649	17	0.400	253.219
3	0.020	190.158	18	0.500	254.273
4	0.025	195.667	19	0.600	255.326
5	C.030	201.176	20	0.700	256.379
6	0.040	205.009	21	0.850	257.453
7	C.050	207.046	22	0.900	258.486
8	0.060	209.082	23	1.000	259.539
9	0.070	211.119	24	1.500	263.699
10	C.085	214.174	25	2.000	260.830
11	J.090	215.192	26	2.500	257.961
12	C.100	217.239	27	3.000	255.092
13	0.150	227.411	28	4.000	249.353
14	0.200	237.594	29	5.000	245.622
15	0.250	247.777	30	6.000	243.287

THICKNESS	150.00	MB TO	100.00	MB =	2398.78	METERS
THICKNESS	1000.00	MB TO	150.00	MB =	13800.87	METERS
THICKNESS	200.00	MB TO	100.00	MB =	4176.99	METERS
THICKNESS	1000.00	MB TO	200.00	MB =	12022.65	METERS
THICKNESS	250.00	MB TO	100.00	MB =	5520.17	METERS
THICKNESS	1000.00	MB TO	250.00	MB =	10579.47	METERS
THICKNESS	300.00	MB TO	100.00	MB =	6847.91	METERS
THICKNESS	1000.00	MB TO	300.00	MB =	9351.74	METERS
THICKNESS	400.00	MB TO	100.00	MB =	8882.28	METERS
THICKNESS	1000.00	MB TO	400.00	MB =	7317.38	METERS
THICKNESS	450.00	MB TO	100.00	MB =	9751.45	METERS
THICKNESS	1000.00	MB TO	450.00	MB =	6448.21	METERS
THICKNESS	500.00	MB TO	100.00	MB =	10546.50	METERS
THICKNESS	1000.00	MB TO	500.00	MB =	5653.14	METERS
THICKNESS	550.00	MB TO	100.00	MB =	11279.45	METERS
THICKNESS	1000.00	MB TO	550.00	MB =	4920.20	METERS
THICKNESS	600.00	MB TO	100.00	MB =	11960.66	METERS
THICKNESS	1000.00	MB TO	600.00	MB =	4238.96	METERS
THICKNESS	650.00	MB TO	100.00	MB =	12597.62	METERS
THICKNESS	1000.00	MB TO	650.00	MB =	3602.02	METERS
THICKNESS	700.00	MB TO	100.00	MB =	13196.45	METERS
THICKNESS	1000.00	MB TO	700.00	MB =	3003.20	METERS

LEVEL	PRESS	TEMP
31	7.000	240.953
32	8.500	237.450
33	9.000	236.283
34	10.000	233.948
35	15.000	228.485
36	20.000	223.442
37	25.000	220.673
38	30.000	218.116
39	40.000	213.197
40	50.000	208.588
41	60.000	204.171
42	70.000	201.706
43	80.000	199.241
44	85.000	198.009
45	90.000	196.777

LEVEL	PRESS	TEMP
46	100.000	197.894
47	150.000	206.133
48	200.000	215.958
49	250.000	225.685
50	300.000	234.192
51	400.000	248.748
52	450.000	255.214
53	500.000	260.133
54	550.000	265.053
55	600.000	269.624
56	650.000	273.822
57	700.000	278.019
58	850.000	281.636
59	900.000	290.636
60	1000.000	299.900

SAMPLE OUTPUT FROM THICKNESS PROGRAM

LIST OF REFERENCES

1. Committee on Extension to the Standard Atmosphere, U.S. Standard Atmosphere Supplements, U.S. Government Printing Office, Washington, D.C., 1966.
2. Crow, E.L., Davis, F.A., and Maxfield, M.W., Statistics Manual, p. 169-179, U.S. Naval Ordnance Test Station, China Lake, California, 1955.
3. Dixon, W.J., Biomedical Computer Programs, p. 305-332, Los Angeles Health Sciences Computing Facility, University of California, Los Angeles, 1966.
4. Drayson, S.R., "Transmittances for Use in Remote Soundings of the Atmosphere," Space Research XI; COSPAR, Plenary Meeting 13th, and Symposium on Remote Sounding of the Atmosphere Leningrad, USSR, May 20-29, 1970, Proceedings, Vol. 1, Akademie Verlag, Berlin, CDR, 1971.
5. Fleming, H.E., "A Method for Calculating Atmospheric Thicknesses Directly from Satellite Radiation Measurements," Conference on Atmospheric Radiation, August 7-9, 1972, Fort Collins, Colorado, Preprint Vol., p. 134-137, AMS, 1972.
6. Fritz, S., Wark, D.Q., Fleming, H.E., Smith, W.L., Jacobowitz, H., Hilleary, D.T., Alishouse, J.C., "Temperature Sounding from Satellites," NOAA Technical Report NESS 59, p. 1-47, Washington, D.C., 1972.
7. Haltiner, G.J., and Martin, F.L., Dynamical and Physical Meteorology, p. 48, McGraw-Hill, 1957.
8. Hayden, C.M., "On Reference Levels for Determining Height Profiles from Satellite-Measured Temperature Profiles," NOAA Technical Memorandum NESS 32, p. 9-10, Washington, D.C., 1971.
9. Holl, M.M., Bibbo, J.P. and Clark, J.R., "Linear Transforms for State-Parameter Structure," Meteorology International Incorporated, 2nd ed., 1964.
10. Jastrow, R. and Halem, M., "Accuracy and Coverage of Temperature Data Derived from the IR Radiometer on the NOAA 2 Satellite," Journal of the Atmospheric Sciences, Vol. 30, No. 6, p. 958-964, 1973.

11. Kaplan, L.D., "Inference of Atmospheric Structure from Remote Radiation Measurements," Journal of the Optical Society of America, Vol. 49, No. 10, p. 1004-1007, 1959.
12. Martin, F.L., Retrieval Procedure of VTPR Radiances Directly in Terms of Thicknesses in such a way as to Optimize Accuracy of Tropospheric Thickness-Values, Research project proposal, Naval Postgraduate School, Monterey, 1973.
13. McCalla, T.R., Introduction to Numerical Methods and FORTRAN Programming, p. 90-92, Wiley, 1967.
14. McMillin, L.M., (Personal Communication), 1973.
15. McMillin, L.M., Wark, D.Q., Siomkajlo, J.M., Abel, P.G., Webowetski, A., Lauritson, L.A., Pritchard, J.A., Crosby, D.S., Woolf, H.M., Luebbe, R.C., Weinreb, M.P., Fleming, H.E., Bittner, F.E., Hayden, C.M., "Satellite Infrared Soundings from NOAA Spacecraft," NOAA Technical Report NESS 65, p. 1-112, Washington, D.C., 1973.
16. Smith, W.L., "Iterative Solution of the Radiative Transfer Equation for the Temperature and Absorbing Gas Profile of an Atmosphere," Applied Optics, Vol. 9, No. 9, p. 1993-1999, 1970.

INITIAL DISTRIBUTION LIST

	No. Copies
1. Defense Documentation Center Cameron Station Alexandria, Virginia 22314	2
2. Library, Code 0212 Naval Postgraduate School Monterey, California 93940	2
3. Professor Frank L. Martin, Code 51Mr Department of Meteorology Naval Postgraduate School Monterey, California 93940	6
4. Lieutenant Douglas R. Moran U.S. Fleet Weather Central, Guam Box 12 COMNAVMARIANAS FPO San Francisco, California 96630	2
5. Department of Meteorology, Code 51 Naval Postgraduate School Monterey, California 93940	3
6. Naval Weather Service Command Naval Weather Service Headquarters Washington Navy Yard Washington, D.C. 20390	1
7. Naval Oceanographic Office Library, Code 3330 Washington, D.C. 20373	1
8. Capt. Hamilton, USN Environmental Prediction Research Facility Monterey, California 93940	1
9. Capt. W. S. Houston, Jr., USN Fleet Numerical Weather Central Monterey, California 93940	1

REPORT DOCUMENTATION PAGE		READ INSTRUCTIONS BEFORE COMPLETING FORM
1. REPORT NUMBER	2. GOVT ACCESSION NO.	3. RECIPIENT'S CATALOG NUMBER
4. TITLE (and Subtitle) Iterative Retrieval and Statistical Specification of Atmospheric Thicknesses from VTPR Clear-Column Radiance Data		5. TYPE OF REPORT & PERIOD COVERED Master's Thesis; March 1974
7. AUTHOR(s) Douglas Ray Moran		6. PERFORMING ORG. REPORT NUMBER
9. PERFORMING ORGANIZATION NAME AND ADDRESS Naval Postgraduate School Monterey, California 93940		8. CONTRACT OR GRANT NUMBER(s)
11. CONTROLLING OFFICE NAME AND ADDRESS Naval Postgraduate School Monterey, California 93940		10. PROGRAM ELEMENT, PROJECT, TASK AREA & WORK UNIT NUMBERS
14. MONITORING AGENCY NAME & ADDRESS (if different from Controlling Office) Naval Postgraduate School Monterey, California 93940		12. REPORT DATE March 1974
		13. NUMBER OF PAGES 91
		15. SECURITY CLASS. (of this report) Unclassified
		15a. DECLASSIFICATION/DOWNGRADING SCHEDULE
16. DISTRIBUTION STATEMENT (of this Report) Approved for public release; distribution unlimited.		
17. DISTRIBUTION STATEMENT (of the abstract entered in Block 20, if different from Report)		
18. SUPPLEMENTARY NOTES		
19. KEY WORDS (Continue on reverse side if necessary and identify by block number) Clear-Column Thickness RMS errors Iterative Transmittance Radiance VTPR Profile Retrieval Multiple Regression		
20. ABSTRACT (Continue on reverse side if necessary and identify by block number) An iterative technique is developed for retrieval of thick- nesses of selected atmospheric layers from VTPR "clear-column" radiance measurements. Layer mean temperatures for a simplified atmospheric model are retrieved by direct solution of the <u>radiative transfer equation</u> , and are then used to compute thicknesses of key atmospheric layers bounded by commonly used pressure levels. The retrieval technique illustrates the use of		

(20. ABSTRACT continued)

reference wave numbers that vary from layer to layer. Transmittance tuning is employed to correct systematic errors in the retrieved mean temperatures. Thicknesses of key layers retrieved by the technique from "clear-column" radiances observed during a 24 hour period at scan spots between 15 N and 45 N are separated into three latitude-band samples. Each sample is subjected to stepwise multiple regression analysis to determine the thickness-specification of various standard layers in terms of the clear column radiances. RMS error-analyses resulting from the regression are then used to determine the quality of thickness-specifications of simulated tropospheres and stratospheres.

